

015089

ANVIL EXPLORATION REPORT

1971 PROGRAM

U. Jansons

D. Jennings

January 21, 1972

Faro, Yukon Territory

TABLE OF CONTENTS

	<u>Page</u>
SUMMARY	i
TABLE OF CONTENTS	vi
LIST OF FIGURES	vii
GEOLOGICAL INVESTIGATIONS	1
GEOPHYSICAL SURVEYS	32
GEOCHEMICAL SURVEYS	35
DIAMOND DRILLING - 1971	43
ASSESSMENT STATUS OF CLAIMS	47
SUMMARY OF 1971 EXPLORATION BUDGET	48
OUTLINE OF 1972 EXPLORATION PROGRAM	50
APPENDICES	

LIST OF FIGURES

Fig. 1	Regional Geology; 2" = 1 mile	pocket
Fig. 2	Geologic Map of Anvil Open Pit	pocket
Fig. 3	Rock Geometry Produced by D <sub>1</sub> - D <sub>2</sub> Events	Page 8
Fig. 4	Geologic Cross Section, East Wall, Anvil Open Pit	pocket
Fig. 5	Post - D <sub>5</sub> Rock Geometry	Page 11
Fig. 6	Geologic Map of Faro Grid	pocket
Fig. 7	Geologic Cross Section AA', Faro Grid	pocket
Fig. 8	Geologic Cross Section BB', Faro Grid	pocket
Fig. 9	Geologic Cross Section CC', Faro Grid	pocket
Fig.10	Geologic Cross Section DD', Faro Grid	pocket
Fig.11	Geologic Cross Section EE', Faro Grid	pocket
Fig.12	Geologic Cross Section FF', Faro Grid	pocket
Fig.13	Geologic Cross Section GG', Faro Grid	pocket
Fig.14	Geologic Cross Section HH', Faro Grid	pocket
Fig.15	Geologic Cross Section II', Faro Grid	pocket
Fig.16	Geologic Cross Section JJ', Faro Grid	pocket
Fig.17	Geologic Cross Section KK', Faro Grid	pocket
Fig.18	Geologic History, Faro Grid	Page 21
Fig.19	D <sub>1</sub> - D <sub>2</sub> Deformational Models	pocket
Fig.20	Gravity Survey - 1971 Residual Map	Page 34
Fig.21	Copper in Soil	pocket
Fig.22	Lead in Soil	pocket
Fig.23	Zinc in Soil	pocket
Fig.24	Rotary Drill Hole Distribution	pocket
Fig.25	Metal Content in Overburden/Bedrock Material - West Faro Grid and North Half East Faro Grid	pocket
Fig.26	Metal Content in Overburden/Bedrock Material - South Half of East Faro Grid	pocket
Fig.27	Metal Content in Overburden/Bedrock Material - SUN-GAL-TIE and BOB-DY-RICH Claims	pocket
Fig.28	Claim Status Map	pocket

## S U M M A R Y

The 1971 exploration program in the Anvil Range included geological, geophysical, and geochemical studies, in conjunction with rotary and diamond drilling programs. Detailed structural and stratigraphic mapping of the Anvil open pit and Faro grid was initiated to develop geological guides for regional exploration and further geologic studies in the Anvil district. The geophysical work included a gravity survey, which was conducted on the Faro grid to detail an electromagnetic anomaly, and a Turair E-M study, which was only partially completed. Two types of geochemical surveys were conducted - one was a regional soil survey and the other was a regional overburden/bedrock geochemistry program. The drilling programs started with an overburden/bedrock program which was designed to take samples for chemical analysis, and the later phase of drilling was coring of rock on selected target areas. Of the \$478,236 budgeted for 1971 exploration, \$468,745 had been spent by December 31, 1971. An exploration program for 1972 consisting of regional and specific follow-up investigations is presented.

### Geological Investigations:

Detailed mapping of the Anvil open pit and Faro grid defined three main lithologic units in the Eocambrian stratigraphic section on the southwestern flank of the Anvil Arch. In ascending order they are: a) biotite-muscovite schist b) calc-silicate gneiss and c) biotite-muscovite phyllite. Regional investigations in the Anvil district demonstrate that stratabound, lead-zinc deposits occur in graphitic, quartz-rich horizons in both the schist and phyllite units. The Faro orebodies occur in the schist unit; the Vangorda, Swim, Firth and Champ sulfide deposits occur in the phyllite unit.

Five periods of deformation and metamorphism have been recognized in much of the stratigraphic sequence. An early metamorphic foliation,  $S_1$ , paralleling a well developed, compositional banding is cut and folded by a younger, penetrative foliation,  $S_2$ , developed during the most pervasive deformational event ( $D_2$ ). Folding during this event transposed  $S_1$  and coincident banding into parallelism with  $S_2$  on all scales resulting in the apparently simple "layer cake" stratigraphy outlined above. By virtue of this transposition, the present stratigraphic section bears no necessary relation to its original depositional attitude. The remaining three deformational events have been superimposed on the post -  $D_2$  "layer cake" stratigraphy. Each event produced a geometrically and temporally distinct fold generation, principal among which are the fourth generation ( $F_4$ ) folds. Two such structures, the Faro anticline and syncline, fold the entire Eocambrian section on the Faro grid.  $F_4$  folds mapped in the pit are congruent and parasitic to the Faro anticline. The Faro orebodies lie on the southern flank of this fold. A similar  $F_4$  fold, the Vangorda anticline, deforms the phyllite unit between Vangorda and Blind Creeks. The Vangorda and Champ deposits occur on the southern flank of this structure.

Grades of regional metamorphism are dominantly middle amphibolite facies. This assignment is based on phase assemblages developed during the  $D_2$ , regional, dynamo-thermal metamorphism. Rocks near Blind Creek may be transitional to upper greenschist facies.

Bulk compositional data suggest the Eocambrian section in the Anvil district represents a quiet water accumulation of variably calcareous pelitic sediments. Presence of graphite in many parts of the section implies reduced conditions during deposition. A deep, marine basin of mio-geosynclinal character is the most probable depositional environment.

Field associations, ages of metamorphic events and sulfur isotopic data suggest a syngenetic origin for the sulfide deposits in the Anvil district. No genetic relationship between sulfide mineralization and the Anvil batholith is apparent. Original bedding, S<sub>0</sub>, in graphitic, quartz-rich horizons in the schist and phyllite units appears to be the primary, structural control of sulfide deposition.

#### Geophysical Investigations:

Geophysical surveys include a gravity survey on the Faro claims which detailed an airborne electromagnetic anomaly and a Turair E-M survey. Because of the spatial relation of the electromagnetic anomaly to the Faro orebodies, a gravity survey consisting of 324 stations on a 100 x 400 foot grid were metered. Two gravity anomalies, one 0.45 mgal and one 0.35 mgal, were extracted from the residual gravity map which had been prepared by the profile method. The maximum depths to the causative masses were calculated as 450 feet and 250 feet. However, sharp local one point flexures suggest that the depths of the causative masses may have been less than 100 feet and the anomalies were possibly a result of overburden thinning. Three rotary holes were drilled to 400 feet in this area with no density contrasts in the rock.

A Turair survey was initiated but only partially completed because of operational problems. The original survey did not cover the Faro orebodies and the ability of this method to locate orebodies at depth in the Anvil Range is unknown.

### Geochemical Investigations:

Two types of geochemical surveys - one to determine the metal content in soil, and one to determine metal content in overburden and bedrock were conducted in the area bounded by Next Creek to the north west and Blind Creek to the southeast. Geochemical orientation surveys were conducted to evaluate the ability of these programs to detect suboutcropping sulfide mineralization.

The survey of the "B" soil horizon readily outlined known zones and extensions of zones of mineralization as well as areas of anomalous total metal (Pb and/or Zn) in soil. The areas of known or suspected mineralization that were outlined by the Pb and Zn content in soil by the 1971 survey are the Vangorda, Firth, and possibly Champ orebodies. Two areas of anomalous metal content in soil not previously known to be related to mineralization are on the Sun, Tie, Gal claims to the northwest and on the Bob claims to the southeast of the Vangorda orebody. The third area of coinciding Pb and Zn anomalies is on the Bill claims near the confluence of Rose Creek and the North Fork of Rose Creek. In the overburden/bedrock geochemical sampling program, samples were taken in 10 foot intervals and analyzed for the total Cu, Pb, Zn, and Hg content. Three areas, the Faro claims, and claim groups northwest and southeast of Kerr-Addison's Vangorda property were drilled on 1000 x 2400 foot centers. A zone of several spatially closely related holes with anomalous total metal content in overburden and one group of anomalous bedrock samples was found in the Bob-Dy-Rich claim area. Three rotary holes were drilled to a maximum of 430 feet in this area. One hole contained anomalous metal values in bedrock to the bottom of the hole - with one set of values reaching 6000 ppm combined Pb-Zn. This hole may have been drilled to one side of possible sulfide mineralization that is reflected by a gravity anomaly.

### Drilling Programs:

Two different drilling programs were conducted on Anvil and Pelly River Mines' claims in 1971. A rotary drilling program of 206 holes sampled overburden and bedrock material for geochemical analysis.

Following the field programs, diamond drilling of 11 holes tested specific areas and targets of interest. DDH 71-210 intersected 10.5 feet of massive and disseminated sulfides assaying at 6.26% combined Pb and Zn in a zone beneath the Faro orebodies east of zone 3. The other holes encountered no economic mineralization.

Cost of the 1971 exploration program was \$468,745 out of a budget of \$478,236. The monies were spent in the following way:

Contract Gravity	3,240.29
Rotary Drilling and all Related Costs	315,513.66
Consulting	4,937.00
Outside Services	5,412.55
Soil Geochemistry	18,731.95
Camp Costs	27,555.04
Geology	22,195.76
Supervision	17,056.75
Diamond Drilling	49,191.02
Equipment, Fuels, etc.	2,283.69
Accruals	2,629.91

Base maps for plotting geologic data from the 1971 and also from the 1972 exploration will be purchased from the funds left over from the 1971 exploration budget.

The 1972 exploration will include continuation of some programs initiated in 1972 and follow-up of targets delineated by the 1971 exploration program. The soil geochemistry program will be continued from Blind Creek to the southeastern end of the Anvil claim group. Regional geological mapping will first be completed in the area between Next Creek and Blind Creek and then extended southeast of Blind Creek into the Swim Lake area. Follow-up work will be on the overburden geochemical anomalies in the Bob-Dy-Rich claim area, the soil geochemical anomalies on the Sun-Gal-Tie claims, Bill claims, and Bob claims. Work will also be completed on claims outside the main contiguous claim group. This will include geological work on the Crown claims and probably diamond drilling on both the Ram and Ted claims.

## GEOLOGICAL INVESTIGATIONS

### Introduction:

The accompanying report is an attempt to consolidate geologic thinking on rocks of the Anvil district. It is based primarily on field work completed by Anvil personnel during the 1971 exploration season, drawing on other investigations only when necessary. In this vein, it is neither a summary of other work in the district nor a review of stratabound lead-zinc deposits in the Omineca crystalline belt.

Current geological investigations in the Anvil district began with a 100 scale pit mapping program. Information gleaned from this program was fit into a more regional context by mapping the Faro grid area at 400 scale. Overlapping and continuing 1000 scale mapping programs were also begun in the Sun-Tie-Gal and Dy-Rich-Bob claim areas as well as in areas immediately adjacent to the Faro grid (Figure 1). Results of these programs will be reviewed in order of their inception.

### Geology of the Anvil Open Pit:

#### Stratigraphy and Intrusive History:

Detailed mapping in the Anvil pit defined the stratigraphic section given in Table I. The spatial distribution of these units is shown in Figure 2. Stratigraphic top is arbitrarily defined according to unit positions within the Anvil Arch (following precedent set by Templeman-Kluit). Contacts between units are gradational except between pelites and quartzite. For example, the calc-silicate gneiss - biotite-muscovite schist contact is gradational over an interval of 30 + feet. Similarly, the biotite-muscovite schist - muscovite-biotite schist contact occurs in a 50 + foot interval. Sulfide-quartzite contacts are gradational over much more narrow intervals (usually < 2 feet). This gradation between sulfides and quartzite emphasizes the Faro #1 orebody was deposited in a quartzite unit, part overlying and part underlying the sulfide mass (Table I). This quartzite occurs as a unit approximately 200-300 feet below the calc-silicate gneiss in a moderately thick section of muscovite-biotite schists.

# GEOLOGICAL INVESTIGATIONS

## Anvil District

### 1971 Exploration Program

D. S. Jennings

#### Abstract:

Three main lithologic units comprise the Eocambrian section of the Anvil district on the southwestern flank of the Anvil Arch (Figure I). In ascending stratigraphic order they are: a) Biotite-muscovite schist b) Calc-silicate gneiss and c) Biotite-muscovite phyllite. All units have highly variable thicknesses and are grossly conformable to the main penetrative metamorphic foliation,  $S_2$ . Massive stratabound lead-zinc sulfide deposits occur in both the schist and phyllite units. The Faro orebodies were deposited in the the protolith of the schist unit while the Vangorda, Swim, Firth and Champ sulfide bodies were deposited in the phyllite protolith.

Five periods of deformation and metamorphism, in addition to the intrusion of the Anvil Batholith, can be systematically mapped in much of the district. The interrelationship of this complex deformational history and the seemingly simple regional stratigraphy are reviewed. Grades of regional metamorphism encountered thus far are dominantly lower to middle amphibolite facies. Rocks near Blind Creek may be transitional to the upper green-schist facies.

Bulk compositional data suggest the Eocambrian section in the Anvil district represents a quiet water accumulation of variably calcareous pelitic sediments. Presence of graphite in many parts of the section implies reducing conditions during deposition. A deep, marine basin of mio-geosynclinal character is the most probable depositional environment.

Current information suggests a syngenetic origin for the sulfide deposits in the Anvil district. No genetic relationship between sulfide mineralization and the Anvil batholith is apparent. Original bedding,  $S_0$ , in graphitic, quartz-rich horizons in the schist and phyllite units appears to be the primary, structural control of sulfide deposition, emphasizing the need for a thorough understanding of the deformational history of the belt.

The spatial association of sulfides, quartzite, graphitic schist and muscovite-biotite schist and their position relative to the lower calc-silicate gneiss contact should be noted. It is emphasized that all stratigraphic unit contacts are conformable to the main metamorphic foliation ( $S_2$ ) in the pit. This foliation is used as the plane of reference for measuring stratigraphic thicknesses relative to an arbitrarily chosen "top direction" on the southwestern flank of the Anvil Arch. Consequently, the stratigraphic section given in Table I bears no necessary relation to original stratigraphic thicknesses or top directions. It is constructed merely as a working stratigraphic section to assess the current spatial distribution of rock units in the Faro area. Consideration of rock origins will be deferred to a separate section later in this report.

Four rock units intrude metamorphic rocks exposed in the pit. Small, fine grained, dark green, chloritic, metamorphosed andesite dikes are the oldest of the four intrusions since they are the only intrusive units cut by the main metamorphic foliation. These dikes show irregular intrusive contacts, and are volumetrically least important of the four intrusive units. Age relationships of the three remaining units cannot be discerned in the pit.

The hornblende-biotite quartz diorite at the north end of the pit is, volumetrically, the largest intrusive unit exposed. It is a coarse grained, light gray-green diorite with conspicuous phenocrysts of hornblende, biotite and quartz. Joint and fault sets pervade the diorite giving it a prominent blocky surface exposure. Weathering occurs to considerable depths (+ 200 feet) along these fracture sets. The exact nature of the weathering products is unknown at present. Little can be discerned of the diorite's general geometry and genetic relation (if any) to the Anvil Batholith from present exposures in the pit.

The fine grained, gray, biotite diorite dike exposed near the southern margin of the pit is probably related to the main diorite mass just discussed. Although black, pseudo-hexagonal prisms of biotite form the main phenocrysts, small amounts of hornblende are also present suggesting a genetic connection.

TABLE I: Stratigraphic Section Through the Anvil Pit

<u>Top</u>	<u>Unit</u>	<u>Description</u>	<u>Thickness</u>
	Calc-silicate gneiss (2a, b)	Finely banded to lenticularly laminated gneiss made up of alternating, fine grained, light green diopside-quartz-feldspar-calcite bands and dark brown to purplish brown, finely crystalline biotite-muscovite phyllite layers. Unit contains occasional, thin, lenticular, moderately coarse-grained, white marble laminae and is calcareous throughout. Base of unit characterized by disappearance of diopside-rich bands and development of thin chlorite schist and amphibolite units.	>400 feet
	Biotite-muscovite schist with graphitic schist interbands (1a, 1b)	Dark brown, homogeneous, finely crystalline, biotite-rich, laminarly foliated schist with black graphitic schist interbands conformable to $S_2$ in the central portion of the unit. Graphitic schist grades laterally into the biotite-muscovite schist along strike. A staurolite rich zone occurs in the upper portion of the unit beneath the calc-silicate gneiss.	100 feet
	Muscovite-biotite schist (1c)	Silvery gray, coarsely crystalline, strongly schistose, porphyroblastic muscovite - biotite chlorite schist. Shows broad, gradational contact with overlying biotite-muscovite schist and sharp contact with underlying quartzite.	150 feet
	Quartzite	Gray, medium grained, discontinuous, muscovite-pyrite rich quartzite in gradational contact with underlying massive sulfides. Foliation in the quartzite is defined by a preferred orientation of phyllosilicate minerals which parallels compositional banding in the massive sulfides. Quartzite is free of Pb/Zn sulfides	0-15 feet



A small, fine grained, pink quartz monzonite to granodiorite dike is exposed in the northwestern corner of the pit. No physical connection of this dike and the main diorite mass is evident despite their proximity. The dike rocks are heavily altered to a punky mass of pinky-brown clay minerals and relict quartz phenocrysts. This alteration may be due to a reaction between a volatile rich granodiorite melt and the underlying sulfide mass.

#### Deformational History:

Five deformational events are recognized in the metamorphic rocks exposed in the pit. A summary of the features produced during each event is given in Table 2.

The earliest recognizable structural feature is the  $S_1$  foliation which occurs as discreet microlithions between  $S_2$  surfaces. The approximate strike of  $S_1$  is  $120^\circ$ - $150^\circ$  dipping subvertically.  $S_1$  is best preserved in the calc-silicate gneiss and biotite-muscovite schist units in the pit. Where visible, this foliation is defined by a preferred planar orientation of biotite and muscovite suggesting a wide range of formative metamorphic conditions (greenschist to upper amphibolite facies). Laminar to thin compositional banding also parallels  $S_1$ . The significance of this banding and its possible relation to original bedding cannot be deciphered within the confines of the pit.  $S_1$  is best preserved in the hinges of  $F_2$  folds (Table 2) and is transposed parallel to the younger  $S_2$  foliation on the limbs of these folds.

The second deformation,  $D_2$ , produced the main penetrative metamorphic foliation imparting a layered appearance to rocks in the pit. Average  $S_2$  strike is  $110^\circ$  -  $120^\circ$  dipping  $20^\circ$  to  $60^\circ$  southwest. Rock unit contacts are parallel to this foliation as described previously.  $S_2$  cuts  $S_1$  and folds it into recumbent, close to tight slip (passive flow, shear etc.) folds here termed  $F_2$ . In general only limited, mesoscopic examples of this fold generation are evident.  $S_2$  is axial planar to  $F_2$  transposing  $S_1$  parallel to itself on the limbs of these folds. The intersection of  $S_1$  and  $S_2$  in the hinge region defines the  $L_2$  lineation

TABLE 2: Deformational Events and Features Produced in Metamorphic Rocks of the Anvil Pit

<u>Event</u>	<u>Structural Features Produced</u>		
	<u>Planar</u>	<u>Linear</u>	<u>Fold Generation</u>
D <sub>1</sub>	S <sub>1</sub> ; earliest penetrative metamorphic foliation, strike 120°-150°, dip subvertical	None detected	None detected
D <sub>2</sub>	S <sub>2</sub> ; main penetrative metamorphic foliation, strike 110°-120°, dip 20°-60° SW	L <sub>2</sub> ; crenulation lineation parallel to S <sub>1</sub> -S <sub>2</sub> intersection, preserved only on hinges of F <sub>2</sub> folds, trend 120°-150°, plunge shallow to northwest	F <sub>2</sub> ; open to tight, parallel to similar slip folds in S <sub>1</sub> , S <sub>2</sub> axial planar to F <sub>2</sub> , L <sub>2</sub> parallel to F <sub>2</sub> axes
D <sub>3</sub>	S <sub>3</sub> ; weak, non-penetrative metamorphic foliation, strike 150°-160°, dip subvertical	L <sub>3</sub> ; strong, penetrative crenulation lineation parallel to S <sub>2</sub> -S <sub>3</sub> intersection, trend 150°-160° plunge 20°-40° southeast	F <sub>3</sub> ; open to close, parallel flexural slip folds in S <sub>2</sub> , where developed S <sub>3</sub> is axial planar to F <sub>3</sub> , L <sub>3</sub> parallel to F <sub>3</sub> axes
D <sub>4</sub>	S <sub>4</sub> ; weak, non penetrative metamorphic foliation, strike 110°-120°, dip subvertical; series of thrust faults parallel to S <sub>2</sub>	L <sub>4</sub> ; weak, non-penetrative crenulation lineation parallel to S <sub>2</sub> -S <sub>4</sub> intersection, trend 110°-120° plunge shallow northwest or south east	F <sub>4</sub> ; open to close, parallel doubly plunging flexural slip folds in S <sub>2</sub> , where developed S <sub>4</sub> is axial planar to F <sub>4</sub> , L <sub>4</sub> parallel to F <sub>4</sub> axes
D <sub>5</sub>	S <sub>5</sub> ; very weak, non-penetrative metamorphic foliation, strike 60° - 80°, dip subvertical	L <sub>5</sub> ; very weak, non-penetrative, crenulation lineation parallel to S <sub>2</sub> -S <sub>5</sub> intersection, trend 60°-80° plunge shallow northeast or south west	F <sub>5</sub> ; open to close, parallel, doubly plunging flexural slip folds in S <sub>2</sub> , where developed, S <sub>5</sub> is axial planar to F <sub>5</sub> , L <sub>5</sub> parallel to F <sub>5</sub> axes

which parallels a well developed crenulation lineation trending  $120^{\circ}$ - $150^{\circ}$  and plunging shallowly to the northwest. In all probability, this crenulation lineation developed in response to flexural slip (slip along  $S_1$  surfaces) during the beginning of the  $D_2$  event,  $L_2$  is now preserved only in the hinge zones of  $F_2$  folds, since  $S_1$  has been transposed parallel to the developing  $S_2$  foliation in the limbs of these folds as deformation proceeded. Thus,  $D_2$  changed from early active behaviour of  $S_1$  to passive behaviour in the latter stages of deformation.

Both the  $D_1$  and  $D_2$  events have produced penetrative planar and linear features on the scale of the pit. Metamorphism associated with the  $D_1$  event is, at least, of biotite grade and probably higher.  $D_2$  metamorphism is of middle amphibolite facies rank. These events represent the most important dynamothermal metamorphisms recorded in the pit rocks and, for convenience, are referred to as an early deformational package. The metamorphic fabric produced by these events is the frame of reference for measurement of fabrics related to subsequent events. Rock geometry produced by the early deformational package is summarized in Figure 3. Because of their mesoscopic scale, effects of these early deformations are not readily visible in Figure 2. The most obvious feature related to these events is the general parallelism of stratigraphic unit contacts to  $S_1$ . One moderately sized  $F_2$  fold is exposed in quartzites on the 3990 bench, east wall. This fold is refolded about a later  $F_4$  axis.

$D_3$  deformation and metamorphism produced a weak, non-penetrative, metamorphic foliation,  $S_3$ , axial planar to  $F_3$  folds in  $S_2$ .  $S_3$  strikes  $150^{\circ}$  -  $160^{\circ}$  and has a subvertical dip. Its intersection with  $S_2$  is parallel to a penetrative, crenulation lineation,  $L_3$ , trending  $150^{\circ}$ - $160^{\circ}$  and plunging  $20^{\circ}$ - $40^{\circ}$  southwest.  $L_3$  parallels the axes of  $F_3$  folds which are open to close, parallel, flexural slip folds in  $S_2$ . The  $L_3$  crenulation lineation developed in response to interfolia slip along  $S_2$  during the formation of  $F_3$  folds at the beginning of  $D_3$  movement. Toward the end of the  $D_3$  event, phyllosilicates developed parallel to the axial plane of these folds defining  $S_3$ . This developing foliation began to act as the active plane of slip in  $F_3$  folds during the last stages of deformation, but movement ceased before true slip folds developed. Movement along  $S_3$  emphasized the amplitude of the  $L_3$  lineation. A large family of  $F_3$  folds constitutes an important structural feature in the northwestern end of the pit while the  $L_3$  lineation is penetrative in the total volume of pit rocks. The amplitude of  $F_3$  folds in the pit varies from a few inches to approximately 30 feet. Wavelengths of these folds average about 50 feet for

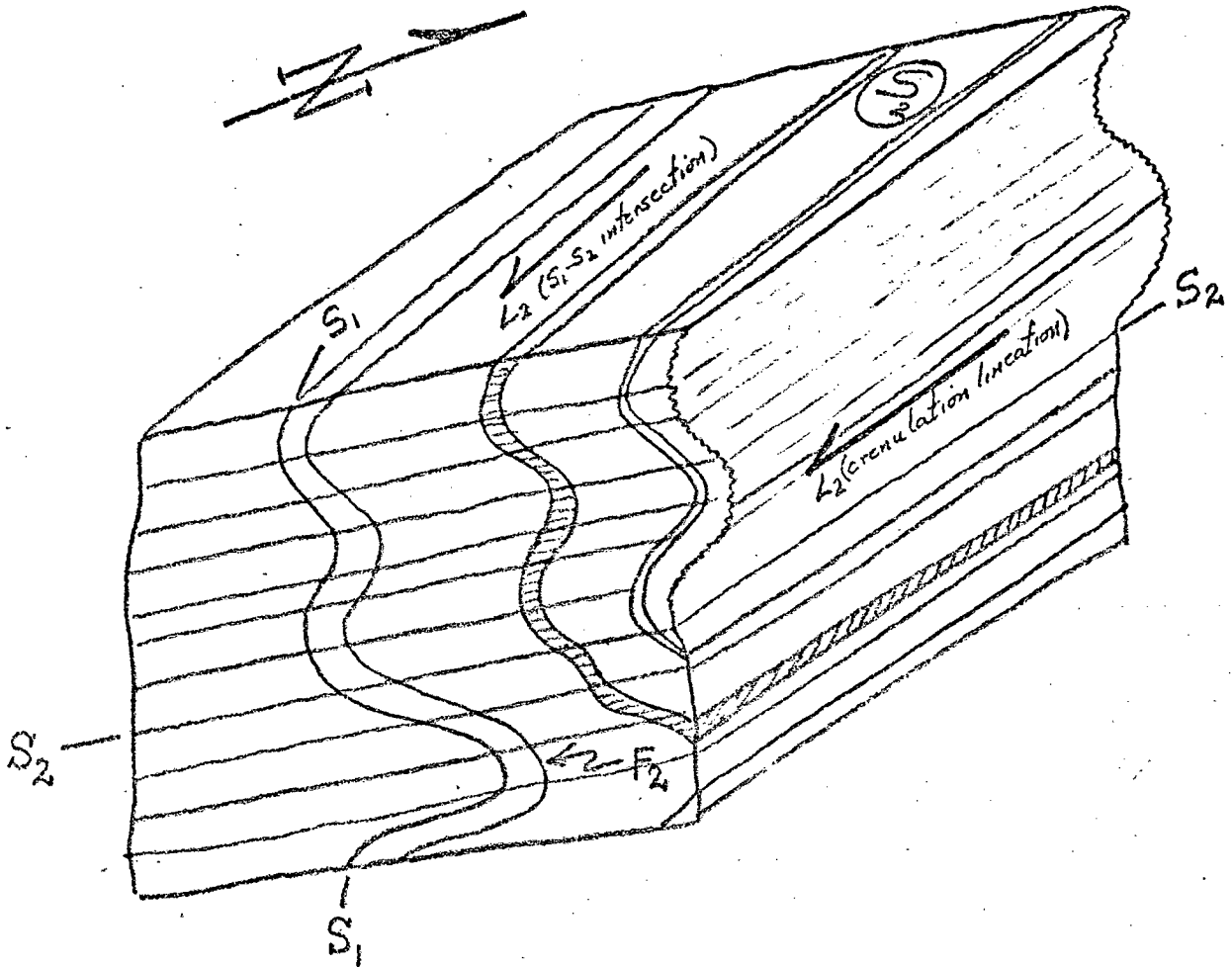


FIGURE 3: ROCK GEOMETRY PRODUCED BY THE  $D_1$  &  $D_2$  EVENTS

the larger folds. Grade of metamorphism associated with the  $D_3$  event is uncertain at present since only biotite and muscovite can be recognized visually as stable minerals in the plane of  $S_3$ .

$D_4$  deformational features superimposed upon the  $D_1$ ,  $D_2$  and  $D_3$  fabrics include a non-penetrative, axial planar, metamorphic foliation,  $S_4$ , striking  $110^\circ$ - $120^\circ$  dipping subvertically; a non-penetrative crenulation lineation,  $L_4$ ; and the open to close, doubly plunging, parallel, flexural slip,  $F_4$  folds in  $S_2$  themselves.  $L_4$  is parallel to  $F_4$  axes; it trends  $110^\circ$ - $120^\circ$  and plunges shallowly northwest or southeast.  $F_4$  folds are genetically similar to those of the  $F_3$  generation and are distinguished by their unique orientation in space and by deformation of the pre-existing  $D_3$  fabric. Folds of this generation are the largest recognized in the pit. Approximate amplitudes of the  $F_4$  folds on the east wall (Figures 2 and 4) are 50-120 feet (increasing northward) with wavelengths of approximately 250 feet. These folds appear to decrease in amplitude rapidly with depth in the exposed portion of the orebody suggesting significantly different mechanical behaviours between the sulfides and country rocks (Figure 4). The doubly plunging character of the  $F_4$  folds in conjunction with their size emphasize their significance to problems of ore control. A tabular sheet of massive sulfides extends upward from the crest of the northernmost anticline on the east pit wall. (Figures 2, 4) Absence of enveloping quartzite and fault contacts with muscovite-biotite schist suggest this sulfide sheet is the remobilized equivalent of the north limb of the fold transported along fault surfaces either during the last stages of  $D_4$  movement or  $D_5$  faulting.

In addition to the folding just described, thrust faulting occurred during  $D_4$  along pre-existing  $S_2$  surfaces. At least six thrusts can be recognized on the west wall of the pit (Figure 2). Slip lines for these thrusts appear to be normal to  $F_4$  axes and  $D_4$  boudin lines indicating a genetic relationship between thrusting and  $F_4$  folding during brittle  $D_4$  deformation. The active character of  $S_2$  during this deformation is emphasized. Allochthonous movement during thrusting has been to the northeast.

$D_4$  metamorphism is, at least, biotite grade. Facies assignment must await petrographic investigation.

Features produced by the  $D_5$  event occur only sporadically in the pit.  $S_5$  is a very weak, non-penetrative, metamorphic foliation of at least biotite grade striking  $60^\circ$ - $80^\circ$  dipping subvertically. It is axial planar to  $F_5$  folds which are geometrically similar to  $F_4$  folds on a much smaller scale.  $F_5$  folds are spatially associated with normal faults cutting the previously described thrust faults. A crenulation lineation,  $L_5$ , is parallel to the axis of  $F_5$  folds. This lineation is produced by flexural slip along  $S_2$  in a manner similar to  $L_3$  and  $L_4$ . It is parallel to the  $S_2$ - $S_5$  intersection.

Perhaps the broad zone of northwest striking normal faults through the center of the pit (Figure 2) developed during the  $D_5$  event. Since this fault set cuts the  $D_4$  thrust faults and  $F_4$  folds, the normal faulting is a very late  $D_4$  or a post- $D_4$  feature. Intrusion of the hornblende-biotite quartz diorite body at the north end of the pit may have created a stress field conducive to normal faulting along its southern margin. Alternatively, relaxation of  $D_4$  compressional stresses may have produced very late  $D_4$  brittle failure along this broad fault zone.

In summary, the early deformations,  $D_1$  and  $D_2$ , are characterized by ductile deformational features. The passive behaviour of older planar anisotropy during slip folding and the development of penetrative metamorphic foliations ( $S_1$  and  $S_2$ ) distinguish the early deformational package from later events. Active behaviour of existing anisotropy ( $S_2$ ) during the  $D_3$ ,  $D_4$  and  $D_5$  events allowed development of flexural slip folds and non-penetrative, axial planar, metamorphic foliations characteristic of this later deformational package. Age relationships in the deformational sequence given in Table 2 were defined by careful observation of cross-cutting structural features. A summary of post- $D_5$  rock geometry is given in Figure 5.

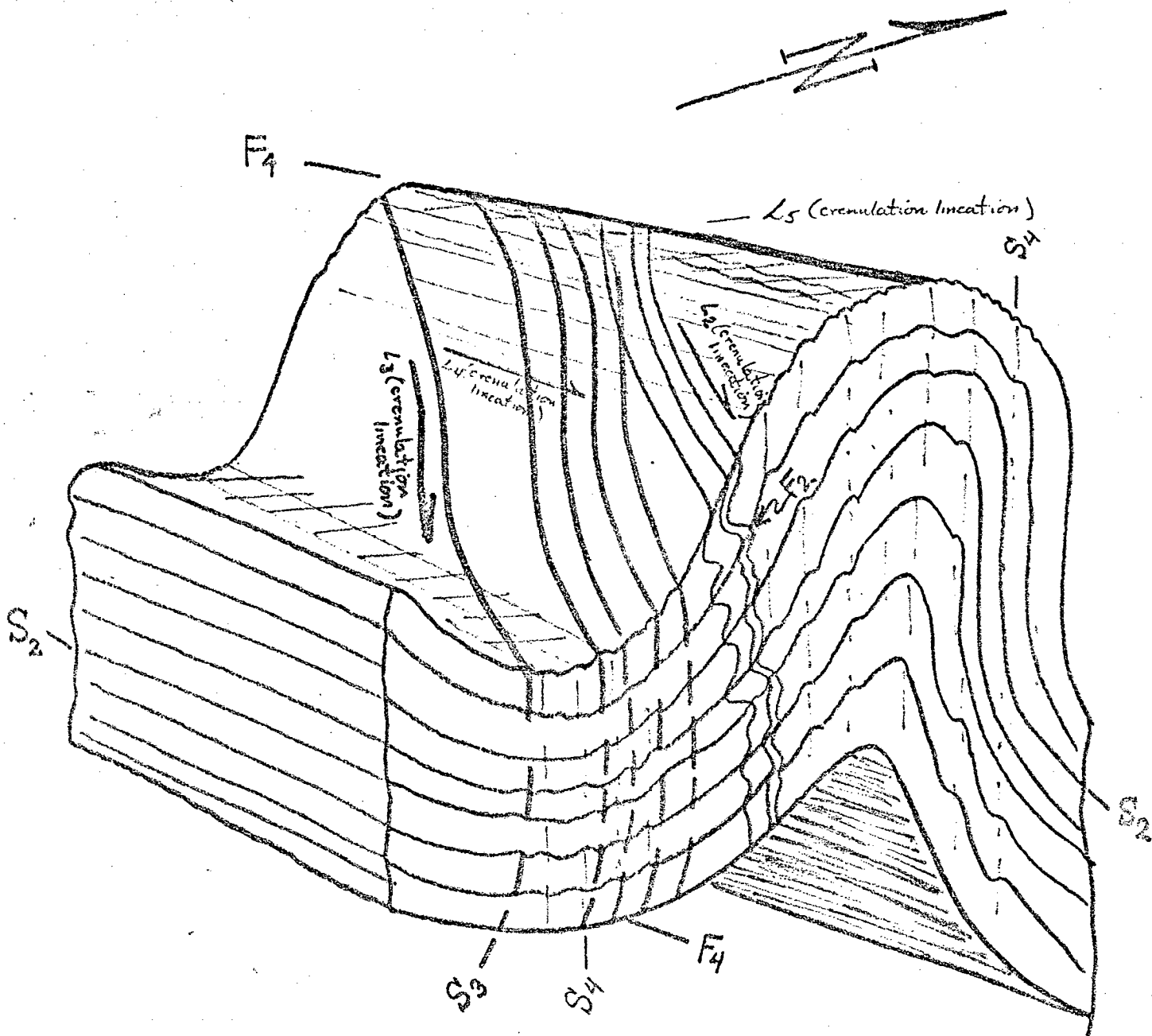


FIGURE 5: POST-D<sub>5</sub> ROCK GEOMETRY (F<sub>3</sub> & F<sub>6</sub> FOLDS OMITTED)

### Relationship of Sulfides to Stratigraphy and Structure:

Massive sulfides in the pit occur within a quartzite unit enveloped by muscovite-biotite schists (Figure 2). The sulfide-bearing quartzite lies 200-300 feet beneath the contact of the calc-silicate gneiss and the graphitic biotite schists. The spatial association of these units must be considered in any model of sulfide genesis; their stratigraphic position within rocks of the Anvil district may be a valid exploration guide.

Five deformational events have been superimposed on the sulfide-bearing sequence. The degree to which sulfides have been transposed from their original depositional attitude into parallelism with  $S_1$  and  $S_2$  is unknown. Folding associated with the  $D_3$ ,  $D_4$  and  $D_5$  events has merely crenulated the sulfide mass which is grossly conformable to  $S_2$ .

### Geology of the Faro Grid:

#### Stratigraphy and Intrusive History:

Detailed 400 scale mapping of the area adjacent to the open pit required expansion of the stratigraphic section recognized in the pit. Above the calc-silicate gneiss unit and in gradational contact with it is a thick sequence of calcareous, gray-brown, fine grained, fissile, biotite-muscovite phyllites (unit 3a, Figure 6). Since the top of this unit is nowhere exposed on the Faro grid, estimates of its true thickness cannot be made at present. The base of the phyllite unit is defined at the uppermost extent of the light green, diopside-rich laminae in the underlying calc-silicate gneiss. Compositionally, the phyllitic partings in the calc-silicate gneiss are very similar to the main phyllite unit.

Since the detailed units underlying the calc-silicate gneiss in the pit (Table 2) cannot be recognized as systematically mappable units on the scale of the grid, they have been included in a biotite-muscovite schist unit (unit lg, Figure 6) which is readily mappable at this scale. It is a coarsely porphyroblastic, silvery grey brown, heavily foliated schist showing variable muscovite-biotite proportions. The base of this unit is not exposed on the grid, thus no reliable estimate of its thickness can be made. The calc-silicate gneiss unit between the schist and phyllite varies in thickness between 600 and 1200 feet. An approximate stratigraphic column for the Faro grid is given in Table 3.

TABLE 3: Stratigraphic Section, Faro Grid

<u>Top</u>	<u>Unit</u>	<u>Thickness</u>
	Biotite-muscovite phyllite -----	> 2000 feet
	Calc-silicate gneiss -----	600-1200 feet
<u>Base</u>	Biotite-muscovite schist ----- = gradational contact	> 2000 feet

As in the case of the pit, the top direction for this section is arbitrarily defined and stratigraphic unit contacts are parallel to the main metamorphic foliation. Since the biotite-muscovite schist is exposed in the core of the Anvil Arch, it is considered the oldest stratigraphic unit on the grid.

The most plausible explanation for the graphitic schists and quartzites not being mappable units in the biotite-muscovite schist is their direct spatial and presumed genetic association with sulfides. In addition, exposure along the belt underlain by the schist unit is not particularly good.

Silicated marble horizons (2b) occur within the calc-silicate gneiss. These marbles may vary from moderately coarsely crystalline, white, essentially pure, carbonate rocks to finer grained, diopside-rich, light greenish gray calc-silicate bands. They vary in thickness from 50 to 150 feet and cannot be traced over distances greater than 1000 feet because of poor exposure.

The biotite-muscovite phyllite (unit 3a) cannot be subdivided on the Faro grid. Sporadic outcrops of an apparently more muscovite-rich phyllite are encountered which may occur as a unit in the phyllite elsewhere.

Fine grained, dark green amphibolites (10a) are the oldest intrusive rocks exposed on the grid. They show intrusive contacts with the enclosing calc-silicate gneisses and are the only intrusive rock type cut by the  $S_2$  foliation. On the basis of their outcrop pattern, these amphibolites are thought to be irregular gabbro plugs or dikes.

Rocks of the Anvil Batholith appear to be the next igneous suite to intrude the Eocambrian metamorphic section. The bulk of the batholithic rocks are coarsely crystalline biotite-quartz monzonites to biotite-granodiorites (11a) with large, characteristic, potassium feldspar megacrysts. The monzonitic and granodioritic rocks show a penetrative foliation defined by the preferred planar orientation of biotite flakes and long axes of the feldspar megacrysts. Within the plane of foliation, the long axes of these megacrysts are randomly oriented. This foliation in all likelihood is an igneous flow foliation since it bears no relation to any foliation in the country rocks. Leucocratic, unfoliated, medium crystalline, hornblende-biotite

diorites (14c) occur as border phases of the batholith at two areas along its contact on the Faro grid (Figure 6). Their genetic relationship to the monzonitic phase of the batholith is unknown at present. Contact metamorphic effects attributable to the Anvil Batholith appear to be negligible, as there is minimal development of hornfels near its contact with the country rocks. Petrographic examination of contact zone rocks will shed further light on this matter.

Coarsely porphyritic, medium to dark green, hornblende diorite dikes (13a) cut the batholithic rocks at several places on the grid. These dikes follow a northeasterly trend and may be intruded along fracture sets produced by intrusion of the batholith. The diorite mass in the north end of the pit is the largest single body in this diorite clan. A narrow (up to 100 feet) zone of contact hornfelsing is developed in the pit rocks adjacent to it. Phase assemblages in the hornfels defining its grade (<sup>s</sup>) of metamorphism have not been worked out.

Intrusion of hornblende diorite in the country rocks around zone 3 produced extensive brecciation (Figure 6). Diorite, seen as the breccia matrix, appears to have exploded its superencumbent cap rocks as volatile pressures associated with the original diorite melt exceeded lithostatic pressures on the melt. Fragments in the breccia vary in size from 1/4 inch to approximately 10 feet on their long dimension. In general, there is very little diorite matrix in the breccia, which, as a result, has the appearance of randomly jumbled, welded blocks of rock. The limits of brecciation are difficult to define because of generally poor exposure. On the basis of surface exposures, brecciation occurs only between the center and north base lines and lines 24 W to 52 W (Figure 6). The age of brecciation is at least that of the D<sub>2</sub> deformation since fabric elements associated with that event are affected by brecciation. A more probable age is mid to late Cretaceous since quartz-monzonite of the Anvil Batholith gives potassium-argon ages of 90-95 m.y. and is cut by the diorites. Moderately large, angular blocks of banded, highly weathered, massive sulfides occur in the breccia near line 36 W between the center and north base lines. These sulfides represent the brecciated northeast extension of zone 3 and will be discussed in a later section.

Another breccia is exposed near the intersection of line 8 W and the North Fork of Rose Creek. The preponderance of fragments in this breccia are calc-silicate gneiss averaging less than 2 feet along their maximum dimensions. Hornblende diorite, again the matrix of the breccia, shows moderate amounts of sphalerite and galena mineralization. A representative analysis of the breccia indicates the following metal values: (not available)

A relatively minor, medium grained, equigranular, dark pink monzonite intrudes the breccia. This phase seems to follow joint surfaces in the existing breccia and appears to be later than the main phase of brecciation. It is unmineralized. Source of the base metals in the diorite is possibly an eastern extension of the Number 2 zone intruded by the diorite. The presence of the calc-silicate gneiss fragments in the biotite-muscovite schist unit remains unexplained. An irregular, subsurface intrusive diorite body centered on line 16 W between the central and south base lines may be the parent of the diorite causing brecciation.

Intrusion of smokey quartz-feldspar porphyry (14b), minor muscovite granite (14a) and leucocratic, tourmaline-garnet monzonite dikes (11b) is the last recognizable intrusive event on the Faro grid. In the absence of definitive cross cutting relationships, intrusion of these granitic rocks is considered to be one event. Since the muscovite granite and monzonite dikes cut hornblende diorite dikes and the porphyry cuts a breccia most probably produced by diorite intrusion, these granitic rocks are considered to be younger than the diorite clan.

In summary, four intrusive rock sequences are recognized on the Faro grid. On the basis of cross cutting relationships, the amphibolites are the oldest recognizable intrusive unit since they are cut by the  $S_2$  foliation ( $D_2$  metamorphism is Ordovician according to Templeman-Kluit).<sup>2</sup> The next recognizable event is the intrusion of the Cretaceous Anvil Batholith. Hornblende diorites intrude the batholithic rocks and brecciate the Eocambrian metamorphic rocks near inferred centers of diorite intrusion. Late stage granitic and monzonitic dikes cut rocks of the diorite clan and breccia produced by it.

### Deformational History:

Rocks on the Faro grid have the same geometry and deformational history as those in the pit. All of the structural features described in the pit, including its deformational history, apply to rocks on the grid.

The  $S_1$  foliation is best developed in the biotite-muscovite phyllite unit. Most phyllite outcrops show well developed  $F_2$  folds in  $S_1$ . In general, these folds are parallel to similar and have sub-equal limb heights.  $S_2$ , the active plane of movement, is axial planar to these folds which are developed on all scales. Commonly  $F_2$  folds have limb heights of fractions of inches to several inches. In large outcrops, limb heights of 10 to greater than 100 feet are observed. These larger scale  $F_2$  folds are not commonly seen because of prevailing small outcrop size.  $S_2$  Thin to laminar compositional banding parallel to  $S_1$  emphasizes  $F_2$  folds in outcrop. Occasionally,  $S_1$  seems to show a consistent attitude in outcrop suggesting either a uniformly dipping, undeformed, penetrative, regional metamorphic foliation or, more likely, a uniformly dipping portion of a large  $F_2$  fold limb. Attitudes of such large planar  $S_1$  surfaces strike  $120^\circ$ - $150^\circ$  and dip sub-vertically. Axes of  $F_2$  folds trend  $120^\circ$ - $150^\circ$  with a cluster around  $140^\circ$  and plunge shallowly  $S_2$  northwest or southeast parallel to the  $L_2$  crenulation lineation. Figure 3 summarizes this geometry.

$F_2$  folds are not as well preserved in the calc-silicate gneiss and biotite-muscovite schist emphasizing the difference in mechanical behaviour of the different stratigraphic units. Since  $F_2$  folds are better preserved in the gneiss than the schist, the latter appears to have behaved in a more ductile manner during  $D_2$ . The gneiss in turn showed more ductile behaviour than the phyllite. The general absence of  $F_2$  folds in the massive sulfides exposed in the pit suggests they have the lowest ductility contrast with other units in the stratigraphic pile.

As in the pit, banding in the calc-silicate gneiss and biotite-muscovite schist parallels the main, penetrative  $S_2$  foliation. Banding in the phyllite only parallels  $S_2$  on limbs of  $F_2$  folds further suggesting its high ductility contrast. In addition, the major stratigraphic unit contacts (or regional compositional banding) parallel  $S_2$  giving rise to a regional "layer cake" stratigraphy. The inferred mechanical behaviour of the different units suggests that compositional banding on

all scales represents  $S_1$  banding variably transposed into parallelism with  $S_2$  by the  $D_2$  deformation. Transposition in the schists was complete, in the gneisses nearly complete, and in the phyllites incomplete.

On the scale of the grid, the  $F_3$  folds and  $L_3$  lineation are the only recognizable  $D_3$  structural features.  $S_3$  is developed sporadically in some mesoscopic  $F_3$  folds.  $L_3$  is penetrative on the scale of the grid and can be recognized in nearly all outcrops.  $F_3$  folds of varying scale occur in all rock types. Macroscopic  $F_3$  folds are developed along the southern margin of the Anvil Batholith on the west grid. These folds are parallel, flexural slip folds overturned slightly to the northeast. Their axes trend  $150^\circ$ - $160^\circ$  and plunge  $10^\circ$ - $30^\circ$  to the southeast. Amplitudes of these structures vary from 100 to 800 feet with wavelengths of 1800 to 3200 feet (Figures 6 and 8). The close spatial association of these folds and the batholith suggests a genetic connection. Inspection of cross-section BB' (Figures 6 and 8) shows that the batholith cuts the  $F_3$  folds making a genetic relationship suspect. It is possible these folds developed in response to initial diapiric upwelling of the batholith which in its later stages of intrusion cut the folds.

$D_4$  features superimposed on the existing poly-deformational fabric include  $F_4$  folds and the  $L_4$  lineation. The  $L_4$  lineation can be found in most outcrops in the gneiss and phyllite units. Because of its coarsely porphyroblastic nature, the muscovite-biotite schist does not preserve this linear feature. Two macroscopic asymmetric, flexural slip, parallel, overturned  $F_4$  folds, termed the Faro anticline and syncline, have been defined on the grid. (Figures 6, 7, 8, 9, 10, 11, 12, 14, 15) These folds in the  $S_2$  foliation give rise to the repetition of stratigraphic units seen on the grid (Figure 6). Their amplitudes are approximately 3000 to 3500 feet over wavelengths of approximately 6000 feet. Axes of these folds trend  $110^\circ$  to  $130^\circ$  and plunge to the northwest on the west grid at about  $20^\circ$ . On the east grid, the axis of the Faro anticline becomes horizontal and the Faro syncline is cut out by the Anvil Batholith. Both folds are overturned to the north on the west grid (Figures 6, 7 and 8). Their sense of overturning and style is identical to that of the  $F_4$  folds in the pit on the south limb of the anticline (Figures 2 and 4). For these reasons, the smaller scale  $F_4$  folds in the pit are considered to be congruent and parasitic to the Faro anticline. The genetic relation (if any)

between these folds and the Cretaceous Anvil Batholith is unclear. Arguments similar to those waged for the  $F_3$  folds and their relation to the batholith could be put forward here as well. In general, these arguments are not compelling since both the  $F_3$  and  $F_4$  fold generations show marked intrusive contacts with the batholith (Figures 6, 7, 8, 10, 11, 12, 14 and 16). In addition, the hornblende diorite body at the north end of the pit cuts the  $F_4$  folds and is probably genetically related to the batholith. Therefore, the  $F_3$  and  $F_4$  folds and the deformational events which produced them are probably pre-Cretaceous in age.

$D_5$  deformational features are seldomly encountered on the Faro grid emphasizing the subsidiary role of this event. Warps in  $S_2$  over the Faro orebodies have geometries similar to  $F_5$  folds but additional work is needed to affirm the connection. Very occasional, mesoscopic  $F_5$  folds are found in the grid rocks and the  $L_5$  lineation is only seen in these instances.

The last recognizable deformational event on the Faro grid is a period of brittle faulting. Two main faults appear to bound the number three orebody on its northwest and southeast margins (Figure 6). The Faro fault is postulated on the northwest to account for large, apparent offsets in the sulfide mass. Movement along this fault is normal with the southeast side downdropped. There is no surface expression of this fault as it occurs in an area of no outcrop. Big Indian's fault bounds zone 3 on the southeast and is, in all likelihood, a right lateral, oblique slip, transcurrent fault. The normal component of its movement produces large, apparent offsets in the sulfide mass by downdropping the northwest block to form a graben over zone 3. The strike slip component of its movement appears to separate zones 2 and 3 (Figures 6, 16 and 17) which, prior to faulting, were probably part of the same sulfide mass. Big Indian's fault is well exposed along line 36 W between the center and north base lines as a mylonite zone 15 to 20 feet in width dipping to the northwest (Figure 6). It cuts an irregular, dike-like mass of smokey quartz feldspar porphyry in this area which is Cretaceous or younger in age. For this reason, faulting is considered the last deformational event in the area. Two minor, left lateral, transcurrent faults subparallel to the Faro fault and Big Indian's fault offset the contact between the gneiss and phyllite units on the west grid.

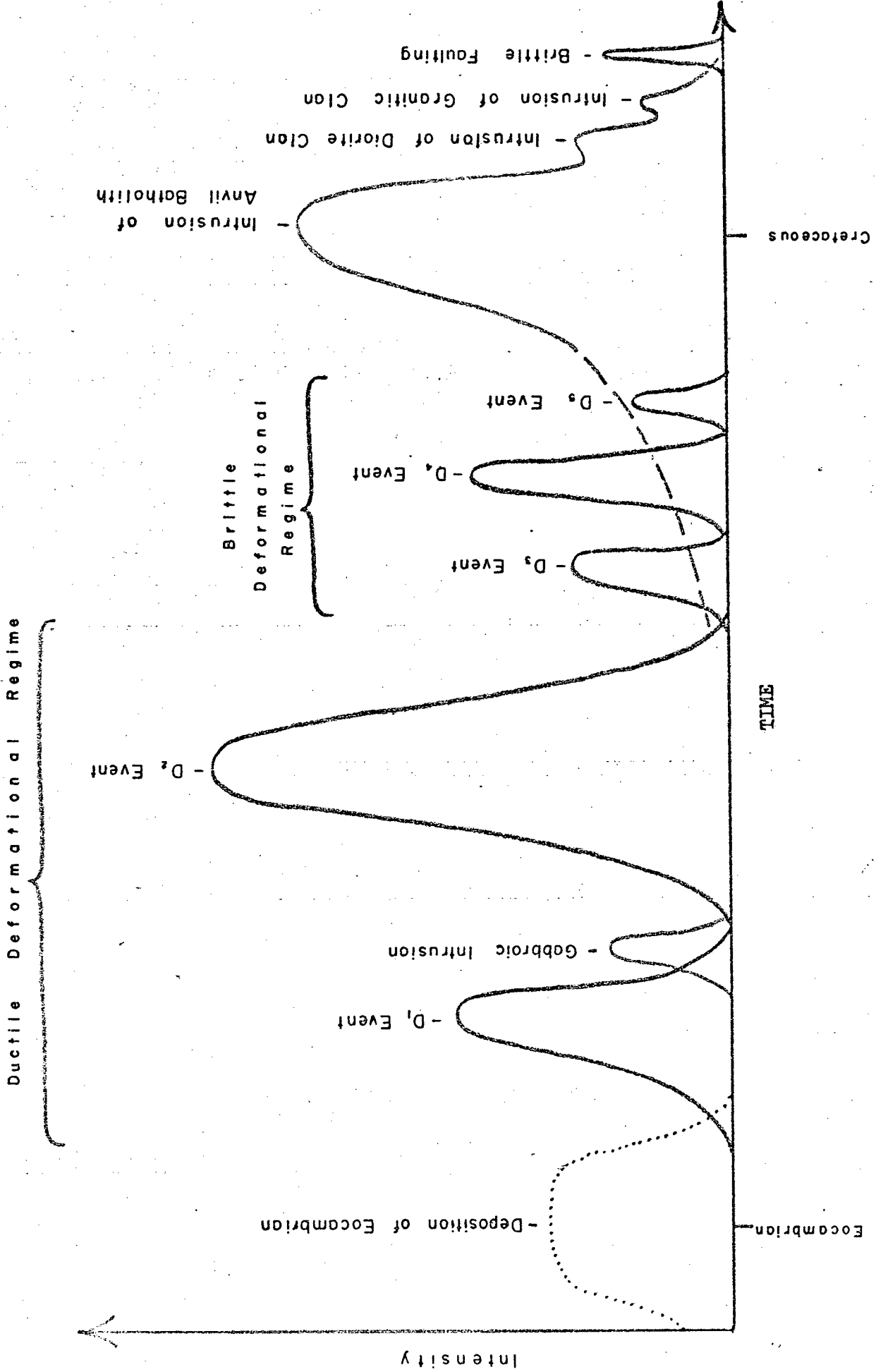
Metamorphism associated with each deformational event is identical to that outlined for these events in the pit. The  $S_1$  and  $S_2$  foliations are penetrative on the scale of the grid.  $D_1$  metamorphism is, at least, biotite grade (lower greenschist facies) and probably higher, while  $D_2$  metamorphism, associated with the main deformational event, is lower to middle amphibolite facies rank. The depositional, deformational and intrusive history of the Faro area is summarized in Figure 18.

#### Relationship of Sulfides to Stratigraphy and Structure:

All lead-zinc sulfide occurrences of note on the Faro grid are found in the biotite-muscovite schist unit approximately 200-300 feet beneath the contact with the overlying calc-silicate gneiss. This interval is characterized by abundant graphitic schist units and is similar to the stratigraphic sequence above the Faro number one orebody as seen in the pit. These relationships provide a valid exploration guide for rocks in the immediate Faro area. Each known occurrence of sulfides in this area will be discussed in this section.

The Faro orebodies are situated on the south limb of the Faro anticline (Figures 6, 9, 10, 11, 12, 13, 14 and 15) in the favourable stratigraphic interval. Section CC' (Figure 9) shows the broad relations of structure in the pit to the Faro anticline.  $F_4$  folds in zone 1 are seen to be congruent and parasitic to the anticline (compare Figures 4, 8 and 9). Extensions of the favourable stratigraphic horizon would logically be expected on the north limb of the anticline. Mapping on this portion of the fold failed to reveal graphitic schist and/or quartzite units. Exploration drilling has confirmed the absence of significant sulfide mineralization in this area but occasional graphitic quartzites have been intersected (DDH 64-D4, Figure 13). These intersections occur 200-300 feet beneath the calc-silicate gneiss suggesting irregular continuations of the favourable horizon across the fold axis.

FIGURE 18: SEQUENCE OF GEOLOGIC EVENT, FARO AREA



Sulfide blocks in the breccia over zone 3 have already been described. Cross section FF' (Figure 12) shows that these blocks are the brecciated, up-dip extension of zone 3 sulfides on the south limb of the Faro anticline.

Banded massive and disseminated sulfides occur in graphitic schists at the top of DDH 71-210 (Figure 6). On the basis of banding conformity to  $S_2$ , the sulfide zone is thought to dip to the southwest in accordance with  $S_2$  in nearby outcrops. Because of their stratigraphic separation from zones 2 and 3, these sulfides are considered to be a separate zone (Figures 13, 14 and 15). Alternatively, they may be an extension of zone 2 which is discordant to  $S_2$  (Figure 15). If this were the case, DDH-71-217 should have intersected sulfides as well. Exploration drilling in the vicinity of this occurrence suggests the sulfides to be of limited extent. Additional definition drilling is proposed.

Sulfide mineralization was also encountered in FRH-2. No structural data could be obtained from the drill log since it was a rotary hole. Consequently, it is not known whether the sulfides encountered were brecciated or not (see Figure 6). Considering the depth of intersection and general structure of the areas, it is simplest to treat this intersection as another zone dipping to the southwest along the south limb of the Faro anticline (Figures 12, 13 and 15). It does not seem likely that sulfides in FRH-2 and DDH 71-210 are related since DDH 71-216, located between them (Figure 6), encountered no mineralization.

The possibility of zones 2 and 3 once being continuous across Big Indian's fault has already been mentioned. Structural relationships in this area are shown in Figures 16 and 17. The broad, open, anticlinal warp in Figure 17 is possibly related to the  $D_5$  event since its axis trends about  $60^\circ$ . Development drilling in this area should clarify the question of sulfide continuity.

Brecciated, massive sulfides are found in the Faro Creek diversion ditch over zone 2 on line 24 W south of the south base line (Figure 6). These sulfide blocks are caught up in a heavily weathered and altered muscovite granite. Cross section JJ' (Figure 16) shows that these blocks were stopped into the granite body as it intruded zone 2 and were transported upward to their present position.

Finely crystalline galena and moderate amounts of marcasite and pyrite have been found in thin quartzites interbanded with graphitic schists southeast of the junction of the North Fork and main tote road. The quartzites and graphitic schists occur a few hundred feet beneath the contact with the calc-silicate gneiss in the biotite-muscovite schist and represent an extension of the favourable stratigraphic horizon enclosing zone 2. While no economic mineralization has been encountered in drilling to date, the occurrence emphasizes the association of mineralization, quartzites and graphitic schists beneath the calc-silicate gneiss.

#### Geological Investigations in Other Areas:

Several areas on the southern flank of the Anvil Arch have been investigated in reconnaissance fashion. These areas include portions of the Ed-Gal-Bill, Sun-Tie-Gal and Dy-Rich-Bob claim groups (Figure 1).

Unit contacts from the Faro grid can be traced into the Ed-Gal-Bill claims (Figure 1). The strong curvature of these contacts reflects the interaction of shallowly dipping stratigraphic units and topography. No fold structures affecting these contacts are mappable in this area. Rock units on this claim group lie on the south flank of the Faro anticline and dip fairly uniformly to the southwest. Features related to at least the  $D_1$ ,  $D_2$ ,  $D_3$  and  $D_4$  events are recognized. One of the most interesting geological features in this area is the presence of moderately thick bands of amphibolite in sharp contact with the biotite-muscovite phyllite. In all probability, the amphibolites are the metamorphosed equivalent of basaltic intrusions or flow rocks. They probably accumulated as an integral part of the stratigraphic sequence and are pre -  $D_2$  in age since they are cut by  $S_2$ .

Mapping on selected portions of the Sun-Tie-Gal and Dy-Rich-Bob claim groups was undertaken to assess the structural and stratigraphic environment of the Vangorda, Champ and Firth sulfide deposits. The areas investigated are underlain by the biotite muscovite phyllite unit (Figure 1). The above-mentioned deposits all occur within this unit and are associated with graphitic horizons. Quartzites and muscovite-rich phyllites are reported to occur with the Vangorda deposit.

The basal portion of the phyllite unit appears to be more muscovite rich and less calcareous than the upper portion and the phyllite unit on the Faro grid. Preliminary whole rock analytical data do not support this contention.

Amphibolite units similar to those encountered on the Ed-Gal-Bill claims are interbanded with the phyllites. Fine grained, gray-green, thinly laminated calc-silicate units commonly envelope the amphibolites. Perhaps these units are metamorphosed tuffaceous horizons associated with basaltic submarine (?) flow rocks now re-crystallized to amphibolites.

Excellent examples of  $S_1$  and  $F_2$  folds are encountered routinely in these rocks. In general, the entire deformational picture for rocks on the Faro grid applies here.  $S_1$  is seen to be transposed parallel to  $S_2$  on the limbs of  $F_2$  folds while remaining relatively undeformed in the hinge zones. In some cases, transposition along  $F_2$  limbs has been severe enough to produce "rootless folds" i.e. detached hinge zones.

The  $L_3$  lineation is probably present in this area, but it may not have the same attitude as seen on the Faro grid. Systematic mapping of the Faro fabric elements from the North Fork to Blind Creek is required to relate rock geometries in the two areas.  $F_4$  folds can be mapped with a fair measure of certainty in the Vangorda area. An overturned anticline-syncline pair occurs on the Sun-Tie-Gal claims while the Vangorda anticline is the dominant  $F_4$  structure on the Dy and Rich claims (Figure 1).

#### Review of Geological Relationships:

Three stratigraphic units have been defined in the Eocambrian sequence in the Anvil district. In ascending stratigraphic order, they are: a) biotite muscovite schist b) calc-silicate gneiss and c) biotite-muscovite phyllite. Five deformational events have

been superimposed on this sequence before intrusion of the Anvil Batholith. The two earliest deformational events occurred at higher grades of regional metamorphism than the latter three. Rocks of the Anvil district behaved in a ductile manner during the  $D_1$  and  $D_2$  events with the production of slip folds and transposition of stratigraphic contacts. The  $D_3$ ,  $D_4$  and  $D_5$  events took place under conditions of brittle behaviour, characterized by the production of crenulation lineations and flexural slip folds. Sulfide deposits associated with quartzites, muscovite schists and graphitic schists occur in the biotite-muscovite schist and biotite-muscovite phyllite; the Faro orebodies occur in the former, Vangorda, Swim, Champ and Firth in the latter.

## Origin of Rock Units:

### Metamorphic Rocks:

The general pelitic bulk composition of the major stratigraphic units leaves little doubt of their sedimentary origin. Known igneous rocks do not show the high  $\text{SiO}_2$  and  $\text{Al}_2\text{O}_3$  contents as well as the high  $\text{K}_2\text{O}/\text{Na}_2\text{O}$  ratios seen<sup>1</sup> in analyses of the main stratigraphic units in the Anvil district. Presence of graphitic schists and quartzites in the schist and phyllite units and marbles in the calc-silicate gneiss lend support to this argument since these inter-banded units are most often developed in sedimentary environments. The most probable mode of accumulation of the entire Eocambrian section is quiet water deposition of pelitic debris in a euxinic marine basin. A marine origin is suspected because of the regional development of the units and their high calcium carbonate content. The schist and phyllite units may represent transgressive sedimentary facies, the calc-silicate gneiss a regressive sequence from a stable, miogeosynclinal shelf environment. Thus, the entire section may represent a sedimentary "off lap" cycle. Graphite in the schist and phyllite units strongly suggests accumulation under reduced conditions in a restricted basin. Source of the carbon may have been decaying algal matter from a proximal carbonate stable shelf area. Quartzites in the schist and phyllite units may be metamorphosed channel fills from the same shelf area. Amphibolites in the phyllites probably represent submarine flows from miogeosynclinal vent centers or island areas.

<sup>1</sup> Thirty whole rock analyses have been completed on rocks from the Anvil district. Accuracy problems preclude their inclusion in this report.

### Sulfides:

A syngenetic model of sulfide accumulation is favoured. The intimate association of sulfides with metasedimentary rocks and their lack of immediate spatial association with intrusive or extrusive igneous rocks suggests sulfide deposition is related to accumulation of the stratigraphic pile. Sulfides in, at least, the Faro number one orebody are stratabound in a quartzite unit. All other occurrences of mineralization in the district are directly associated with graphitic schists. Since quartzites and graphitic schists are almost undoubtedly of sedimentary parentage, the sulfides are considered syngenetic. Sulfur isotopic data shows similar isotopic fractionation between sulfur in the Faro orebodies and sulfur in Cambrian sea water sulfate suggesting sulfur, in at least the Faro deposits, was derived from sea water. At any rate, the observed fractionations in the Faro sulfides bear no resemblance to those in hydrothermal deposits. A sea water source for sulfur complements a syngenetic depositional model. The reduced depositional environment inferred for the graphitic portions of the stratigraphic section fits with the need to reduce sea water sulfate to the sulfide radical.

Regional geologic studies militate against sulfides being related to the Anvil Batholith on several grounds. There is no convincing spatial association of batholithic rocks with any sulfide deposit in the district. In fact, hornblende diorites, presumably a late stage intrusive phase of the batholith, cut Faro number one implying the sulfides are older than, at least, the diorites. Batholithic rocks have been shown to cut fold structures affecting Faro zone 1 further demonstrating the older age of the sulfides (Figure 8). Mapping in the district by Templeman-Kluit has shown that the fabric produced, by what is here termed the D<sub>2</sub> event, is not developed in rocks younger than Ordovician age. Since this event affects all the known sulfide deposits in the district, they must be at least Ordovician. Potassium-argon methods date the Anvil Batholith as mid-Cretaceous.

For these reasons, sulfide deposits in the Anvil district are thought to be syngenetic and Eocambrian in age. Because of the large concentrations of base metals as discreet deposits, rapid accumulation of sulfides is indicated. Rapid accumulation implies either high rates of base metal input into the depositional environment or conditions of sea water saturation with respect to lead and zinc. Lead-zinc rich volcanic exhalations or erosion of pre-existing sulfide deposits could provide base metal sources in either manner to combine with sulfur reduced from sea water sulfate.

Implications of Sulfide Origin and Deformational History to Exploration:

If a syngenetic origin for the sulfide deposits of the Anvil district is accepted, original bedding,  $S_0$ , in sandstone and carbonaceous shale units in the schist and phyllite protoliths appears to be the primary structural control for localization of sulfide deposition. Thus, it is important to trace the original sandstones (now quartzites) and carbonaceous shales (now graphitic schists) through the deformed metamorphic pile in the Anvil district on a regional scale as well as a local one. Locally, graphitic schists, quartzites and muscovite schists have been traced within a restricted stratigraphic interval of the schist unit on the Faro grid.

Similar intervals in the phyllite unit remain to be defined and traced thru the district along with those in the schist unit. In this connection, understanding the early deformational history of the Anvil belt becomes important in defining at what scale folding may duplicate the stratigraphic section.  $F_3$  and  $F_4$  folding occurs on known scales and can be used to trace stratigraphic horizons. The effects of the  $D_1$  and  $D_2$  events are obscured by these later events. Consequently, less is known about them even though they are responsible for much of the rock fabric in the area. The following paragraphs summarize deformation associated with these early periods of folding and their relevance to exploration.

Possible, post -  $D_2$ , pre -  $D_3$  topologies of  $S_0$  can be determined through consideration of several deformational models based on limiting structural conditions. These conditions are tabulated below:

- 1)  $S_0$  was originally horizontal.
- 2)  $S_1$  is a metamorphic foliation found during  $D_1$  in which, at least, biotite was stable.
- 3) Strong compositional banding (laminar to 1 foot thick) is coincident with  $S_1$ .
- 4)  $F_2$  folds have subequal limb heights.
- 5)  $S_2$  transposes  $S_1$  into parallelism with itself on  $F_2$  fold limbs and is the active,  $D_2$ , deformational element.

- 6)  $S_1$  is subvertical in  $F_2$  fold hinges.
- 7) The main stratigraphic units in the Eocambrian sequence are concordant to  $S_2$  over moderately large areas of the district.
- 8)  $F_3$  and  $F_4$  folds flex  $S_2$  into open to close flexural slip folds.
- 9) The Anvil Arch is a mid-Cretaceous dome in  $S_2$  formed by intrusion of the Anvil Batholith.

Unfolding of the Anvil Arch and the  $F_3$  and  $F_4$  folds results in subhorizontal  $S_2$  and stratigraphic unit attitudes. Assuming that only the  $D_3$ ,  $D_4$ , and  $D_5$  events occur between  $D_2$  and formation of the arch,  $S_2$  must have been subhorizontal after the  $D_2$  event. This condition must then be the end product of any analysis of the  $D_1$  and  $D_2$  events.

Beginning with initial deposition of rock units in the Anvil belt, several deformational paths can be taken by originally horizontal bedding,  $S_0$ , to arrive at this condition. With the onset of  $D_1$  metamorphism,  $S_1$  can either develop parallel or at an angle to horizontal bedding,  $S_0$ . These two alternatives cover all possible attitudes of  $S_1$  development but variable behaviour of  $S_1$  during  $D_1$  deformation is possible. Three illustrative cases will be treated: 1)  $S_1$  develops parallel to  $S_0$  2)  $S_1$  develops at an angle to  $S_0$  with minimal transposition of  $S_0$  and 3)  $S_1$  develops at an angle to  $S_0$  with considerable transposition of  $S_0$ . These cases are diagrammed in Figure 19. In each case,  $S_2$  must have a subhorizontal attitude after the  $D_2$  event and resultant rock geometry must satisfy all the limiting conditions in the above list.

Case 1:

$S_1$  develops parallel to  $S_0$  as a bedding plane foliation of, at least, biotite grade during  $D_1$ .<sup>0</sup> This is the most specialized case for  $S_1$  development. If  $S_2$  is constrained to a subhorizontal attitude after the  $D_2$  event, it must be subparallel to  $S_1$  and  $S_0$ . Clearly this violates conditions 4, 5 and 6 since no  $F_2$  folds<sup>0</sup> would ever be produced.

Templeman-Kluit considers  $S_1$  a bedding plane foliation as in this model, but treats  $S_2$  as though it dipped at a moderate angle to the southwest during  $D_2$ .<sup>2</sup> In this way,  $S_2$  folds  $S_1$  and  $S_0$  into  $F_2$  folds with unequal limb heights. His model is at odds with the probable subhorizontal attitude of  $S_2$  prior to doming of the Anvil Arch. It appears as though he used the post-Cretaceous attitude of  $S_2$  on the south flank of the arch and related  $D_2$  deformation to that attitude. Even if  $S_2$  did dip gently to the southwest,  $F_2$  folds in  $S_2$  and  $S_0$  produced by active slip along  $S_2$  would have unequal limb heights contravening condition 4. Templeman-Kluit's model is included in Figure 19 for comparative purposes.

Case 2:

$S_1$  develops at an angle to  $S_0$  producing  $F_1$ <sup>1</sup> folds with minimal transposition of  $S_0$  into parallelism with the axial planar  $S_1$  foliation. Recrystallization of  $S_0$  results in the production of laminar banding parallel to  $S_1$  by "metamorphic differentiation."  $S_2$  creates mesoscopic  $F_2$  folds on the limbs of larger  $F_1$  folds (i.e. in  $S_0$ ) and in the  $S_1$  foliation. This model meets all the required conditions<sup>0</sup> and is attractive in that it requires essentially no bedding transposition, allowing regional conformity of stratigraphic unit contacts to  $S_2$  and original bedding.

<sup>1</sup>  $F_2$  folds are slip folds in  $S_0$  to which  $S_1$  is probably axial planar. They are not seen in rocks of the Anvil district.

This model is not without problems. If "metamorphic differentiation" did occur during  $D_1$  recrystallization, in all likelihood, bedding transposition would have occurred under these ductile conditions as well. In addition, it is doubtful that "metamorphic differentiation" could produce compositional banding at the scales observed under the grades of metamorphism experienced during  $D_1$ . This model would also permit preservation of large numbers of  $F_1$  folds which are not seen in rocks of the Anvil district.

### Case 3:

$S_1$  develops at an angle to  $S_0$  producing  $F_1$  folds with large amounts<sup>1</sup> of bedding transposition parallel to the axial planar  $S_1$  foliation.  $F_2$  slip folds produced during  $D_2$ , refold the  $F_1$  generation folds obliterating their hinges and transposing  $S_1$  and  $S_0$  parallel to  $S_2$ . This model satisfies all the limiting conditions and fits the observed mechanical behaviour of rocks in the Anvil area. It is proposed as a working model of regional  $D_1$  and  $D_2$  deformation subject to revision with additional work.

If the deformational model proposed as Case 3 is correct, exploration implications become apparent. Macroscopic  $F_2$  nappe structures could exist on all scales in the Anvil metamorphic belt. If the stratigraphic unit shaded in Case 3, Figure 19, is considered to be a favourable, quartz-rich graphitic schist horizon, knowledge of its topology increases exploration potential in areas of nappe development.

## GEOPHYSICAL SURVEYS

Geophysical surveys conducted in the 1971 exploration program were gravity and turair.

### Gravity Survey

A gravity survey was carried out to test an E-M anomaly detected by the original Lockwood airborne survey on the Faro claims. This airborne anomaly and its relationship to the Faro #1 orebody and the residual gravity results are shown on Figure 20. The original Faro grid system was used for the gravity survey. A total of 324 stations were metered by Airborne Gravity and Seismic Surveys of Calgary, Alberta. The stations were spaced on 100 foot centers on lines spaced 400 feet apart.

A residual gravity map was prepared from a Bouguer map by the profile method. The following data were extracted from this residual gravity map.

A residual high trend extends from 27S on line 168W across the area to 12S on line 136W. Local closures on this trend exist on lines 156W, 148W, and 140W. Maximum relief is on line 156W (station 17S), but it is only 0.45 mgal, and flank gradients are relatively flat. Maximum possible depth of causative mass from flank gradient and amplitude, were computed at two places and values of 250' and 450' were obtained. However, sharp, one point flexures noted locally, suggest that depth of causative mass actually may be less than 100'. Another residual high was found at 8S on line 166W. Here again, amplitude is only 0.35 milligal and depth of source is thought to be shallow.

The following conclusions and recommendations were presented by R. B. Galeski of Airborne Gravity and Seismic Surveys:

1. It is thought that the residual highs mapped are more likely due to thinning of surface overburden rather than to the presence of orebodies.
2. However, the latter possibility cannot be definitely eliminated.

3. No other evidence of the existence of an orebody was found.
4. It is not recommended that any anomaly shown here be drilled, unless it is backed up by other geological or geophysical evidence.
5. If drilling is to be done, recommended location is a 17S on line 156W.

### Turair Survey

The Turair survey proposed for the Anvil claims was only partially flown due to problems involving the ground loop. No data were recovered directly over the Faro orebodies and the usefulness of this technique for prospecting for sub-surface orebodies in the Anvil Range has not been tested.

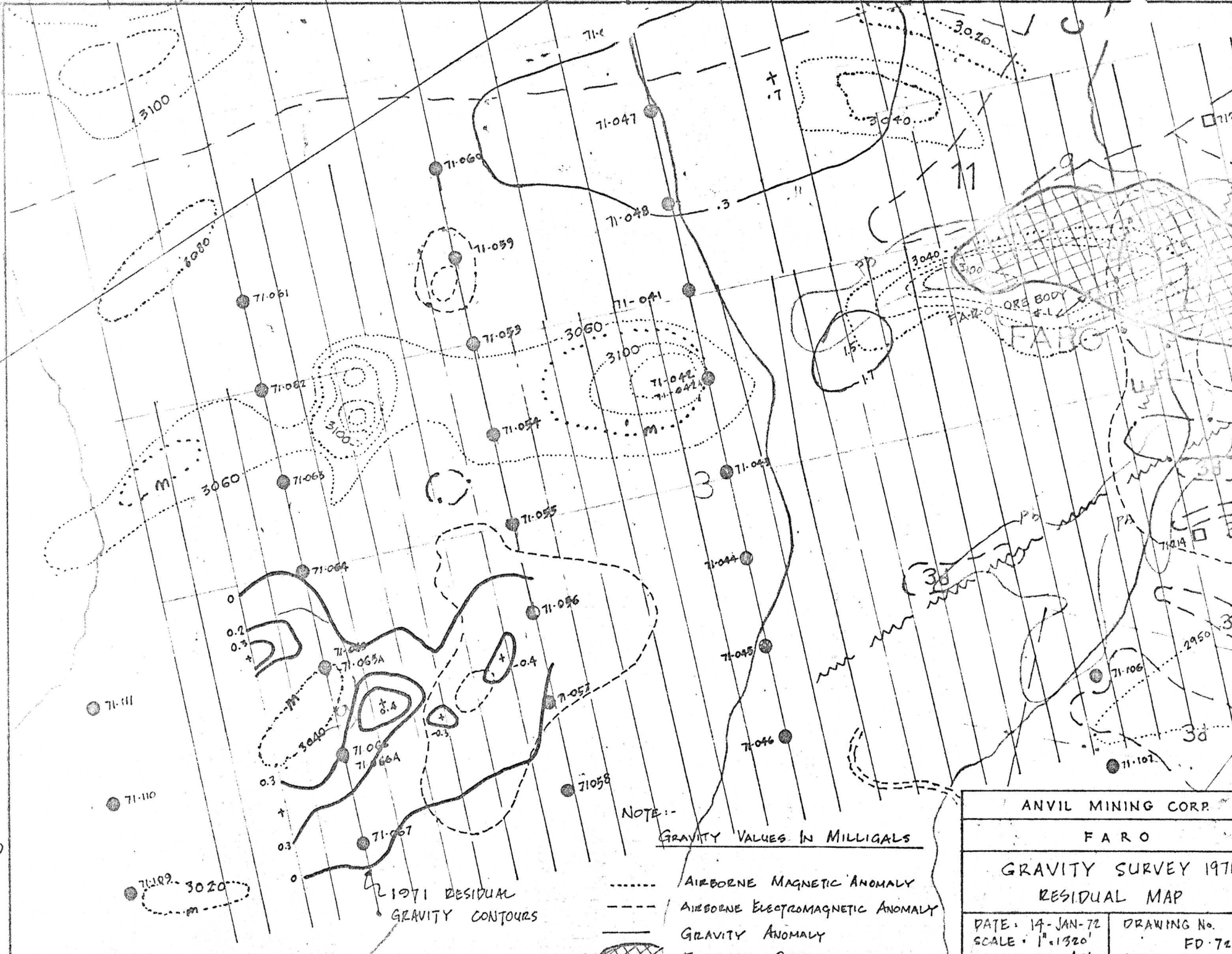
The Turair system was also flown over the Vangorda sulfide deposit to test the system. This was done at no cost to Anvil. No written results have been made available by the contractor. Discussion with the contractor's personnel indicated that the electrical signal decayed rapidly within a short distance of the ground loop. This rapid decay of the electrical field was attributed to the high electrical conductivity of the rocks. This rapid lateral decay of the electrical signal, if in fact due to rock conductivity, would negate one of the main advantages of the Turair system - which is the ability of covering large areas of ground rapidly.

GEOCHEMICAL SURVEYS


Geochemical prospecting included soil sampling and overburden and bedrock sampling for chemical analysis. These samples were analyzed for their total Cu, Pb, Zn, and Hg content to delineate areas of anomalous metal content.

Detailed orientation programs have been performed for soil, overburden and bedrock materials to determine the reliability of sampled materials, the analyzed elements, as well as possible "pathfinder" elements to indicate positions of concentrations of sulfide masses. This orientation study is presented in detail as Appendix I. Conclusions reached in the orientation for the various materials sampled are:

- 1) In soils, the elements As, Cd, Cu, Hg, Pb, and Zn were concentrated in anomalous amounts (A<sub>1</sub> soil, till, and moss samples) near known suboutcropping mineralization and all should be effective in locating mineralized zones in areas with as much as 60 feet of overburden. Lead, zinc, cadmium, and probably arsenic were more specific than other elements in outlining the mineralized zones than the other elements investigated.
- 2) In overburden drilling a direct relationship is observed between continuous intercepts of anomalous metal content in sample material and a nearby source of the metals. Several patterns in the values have been observed at the Faro #2 orebody. Vertically the metal values decreased over a distance of 60 feet from 47300 ppm combined Pb and Zn at the bottom to 1054 ppm combined Pb and Zn at the surface. Uphill from the orebody, the overburden samples contain anomalous amounts of metals but in no apparent systematic distribution. Downhill from the Faro #2 orebody anomalous values were detected in the overburden samples. A systematic decrease in metal values is revealed in two holes, one 500 feet and the second 1000 feet below the Faro #2 zone.
- 3) The bedrock orientation survey of the Faro mineralized zones revealed similar overall average metal contents as detected in analyses of individual rock types. However, a larger spread of values and higher threshold are



NOTE:-  
GRAVITY VALUES IN MILLIGALS

- AIRBORNE MAGNETIC ANOMALY
- - - - - AIRBORNE ELECTROMAGNETIC ANOMALY
- GRAVITY ANOMALY
-  FARO #1 OREBODY

ANVIL MINING CORP.	
F A R O	
GRAVITY SURVEY 1971 RESIDUAL MAP	
DATE: 14-JAN-72	DRAWING No.
SCALE: 1"=1320'	FD-7201
DRAWN BY: A.M.	FILE: W-1

1971 RESIDUAL  
GRAVITY CONTOURS

indicated in areas of known mineralization. Areas of high metal content in bedrock with values in excess of 94 ppm Cu, 185 ppm Pb, and 750 ppm Zn should be considered anomalous based on the data obtained at the Faro orebodies.

- 4) Analysis of metal contents in specific rock types reveals that the Cu, Pb, and Zn contents are nearly identical in all. Because of the similar metal content in the various rock types, systematic differences in the metal content in the soil overlying specific rock types should not vary markedly.

#### Soil Geochemistry

A soil sampling program was initiated in 1971 to cover all contiguous claims from Next Creek to Blind Creek held by Anvil Mining Corporation Limited and by Pelly River Mines Limited. In addition to the regional program two areas in the Faro claim were selected for detailed sampling.

The regional sampling program consisted of taking "B" horizon soil on 200 foot stations along lines spaced 1200 feet apart. A total of 4423 samples were taken, representing 167 miles of sampling. The chemical content of the alternate station samples, those forming 400 foot grid stations on lines spaced 1200 feet apart, was determined by Barringer Research Limited at Whitehorse, Y.T. and Vancouver, B.C. The total copper, lead and zinc content was determined in the -80 mesh fraction by use of perchloric acid sample digestion and atomic absorption spectro-photometric procedures. The average metal value in soils was calculated as 29 ppm Cu, 33 ppm Pb, and 84 ppm Zn.

The metal content of the soil samples was plotted on a regional map at a scale of 1" = 1320'. The metal values on this map were grouped by contouring at intervals of 2-3, 3-4, and greater than 4 times the arithmetic average of the metal content in soil.

### Copper in Soil

The total copper content in the "B" soil horizon soil was contoured at 58 ppm, and 116 ppm levels. The distribution of copper in soil is shown on Figure 21. The largest areal concentration of anomalous copper values is located on the Gal-Ed claims. These values are spatially closely related to the contact between the Upper Paleozoic and the underlying Lower Paleozoic metamorphosed phyllites, schists, greenstones, and calc-silicates. Other areas of anomalous copper content in soil are apparently randomly distributed and generally one, two, or three station anomalies. No groupings in these apparently randomly distributed anomalies contain more than three stations of values greater than three times the arithmetic average. The three station anomaly is on the Gal claim near Rose Creek, about 1200 feet southeast from the confluence with the North Fork of Rose Creek.

### Lead in Soil

The total lead content in "B" horizon soil samples was contoured at the 66 ppm, 99 ppm, and 133+ ppm levels. A major northwesterly trending zone of anomalous high lead content in soil was revealed on the Sun, Gal, Tie claims. The distribution of lead in soil is shown on Figure 22. This zone extends from southeast to northwest partially overlapping the known zone of Vangorda sulfide mineralization off the Vangorda property on to the Sun, Gal, and in part on the Tie claims, for a total length of approximately 23,000 feet and approximate average width of 2,000 feet. Of this strike length, approximately 14,000 feet are on Anvil's claims. The lead content in soils is believed to reflect the distribution of the Vangorda mineralized "stratigraphic" horizon. Support for this hypothesis is given by the formation of a "V" in this trend where the southwesterly dipping rocks are cut by Vangorda Creek. Because the rock strata dip more steeply than the stream gradient, the down-stream pattern is developed.

Four areas with anomalous metal content in soil, spatially removed from this major anomaly zone, are also revealed. Two of these have been drilled by Kerr-Addison - one is spatially closely related to the Firth orebody and the second is now on the Bob claims on an area which has been drilled by Kerr-Addison (Prospector's Airways?). This latter area shows gossan in an adjacent stream, and a jasperized rock sample collected from outcrop near one of three drill holes contained more than 2600 ppm lead.

The third zone of anomalous lead content in soil is located between Rose Creek and the minesite-townsite road, approximately 1200 feet southeast from the confluence of Rose Creek and the North Fork of Rose Creek. This same area also contains anomalous copper and zinc in soil.

The fourth zone of anomalous values is at the confluence of Vangorda Creek and Shrimp Lake drainage into Vangorda Creek. A low coincident E-M anomaly would suggest that this may not be a downstream migration of metals. Field investigation of this area may help decipher the source of lead for these anomalous metal values.

#### Zinc in Soil

The total zinc content in "B" horizon soil samples was contoured at 168 ppm, 256 ppm, and 336 ppm levels. The major area of zinc concentration revealed by contouring in soil is the Sun claims. This anomaly is spatially closely related to the Vangorda orebody and appears to trace the northwestward extension of this mineralized zone. Other anomalies of smaller areal extent were also outlined. A three station zinc anomaly is located northeast of Rose Creek between the minesite and townsite approximately 1200 feet to the southeast from the junction of Rose Creek and the North Fork of Rose Creek. Minor sulfide mineralization has been found outcropping in the road cut to the northeast of this anomaly. Limonite is also forming in seeps near the North Fork of Rose Creek in an area on strike of the observed sulfide mineralization. A two station anomaly is spatially closely related to the Firth orebody. Other zinc anomalies are one station highs, when samples more than 4 times the average zinc content are compared.

The remaining one station anomalies appear to be randomly distributed in the area southeast of the townsite road at the junction with the Vangorda-Blind Creek road.

A lack of any clustered anomalous zinc concentrations in samples collected principally on the Gal and Joe claims is striking by comparison with the previously mentioned area around the Vangorda claims.

#### Overburden - Bedrock Geochemistry

A total of 206 holes, numbered from 71-001 to 71-206, were drilled principally by rotary methods to sample overburden and bedrock material for chemical analysis, and also to identify bedrock in areas of limited outcrop. Most of these holes were confined to the area from Next Creek to Blind Creek, but sixteen holes were drilled on claims to the southeast of Blind Creek for assessment purposes.

The drilling between Next Creek and Blind Creek was confined to three general areas which are spatially closely related to known mineralization or are areas of possible on strike extensions of known mineralization. The three selected areas are 1) the Faro claims, 2) Bob-Dy-Rich claims, and 3) Sun-Gal-Tie claims. Zone 1 is in the area surrounding mineralized zones at Faro 1, 2, and 3 orebodies and Vangorda orebody. Within these areas drill holes were on a grid at 1000 foot stations on lines spaced 2400 feet apart. The distribution and spacing of these drill holes and their relation to known mineralization is shown on Figure 24. The drilling program was designed to penetrate through the overburden and through 20-30 feet of bedrock. Samples were taken in ten foot intervals in both the overburden and bedrock. This drilling was initially done with a modified Atlas-Copco overburden drill and a Boyles Bros. model VAG diamond drill was used to core bedrock. This system was replaced by a Mayhew 1000 rotary drill mounted on a Nodwell track vehicle. Details of the drilling methods and procedures are outlined in the drilling supervisor's report presented as Appendix II.

The samples collected in 10 foot intervals were analysed for their total Cu, Pb, Zn, and Hg content. Samples with high metal content were also analysed for the Cd content. Samples containing more metal than twice the arithmetic average in similar samples are defined as anomalous.

Within these three drilled areas most holes encountered anomalous copper, lead, or zinc content in some samples, but not always in continuous intercepts. Highest metal content in continuous samples was encountered in the line of holes across the Faro #2 orebody. The area of next highest values, and also an area of clustering of holes with anomalously high metal content was found on the Bob-Rich-Dy area. The third area of concentrated drilling on the Sun-Tie-Gal claims showed high Cu, Pb, Zn, or Hg content to the west of the Vangorda claim group and the Vangorda sulfide body. The results of each of the drilled areas are presented in detail. See Figure 24 for rotary hole distribution and Figures 25, 26, 27 for metal content in overburden/bedrock samples.

#### Faro Grid

Overburden bedrock geochemistry on the Faro grid is sub-divided on basis of areal distribution into two groups for discussion. These areas are 1) the West Faro grid - the area northwest of grid line 64W, and 2) the East Faro grid to the southeast of grid line 64W.

On the West Faro grid, the area northwest of line 64W, which approximately defines the boundary between the Faro 1 and Faro 3 orebodies, contains rotary drill holes with continuous interval of anomalous metal content in overburden for thirty or more feet. Four of these holes, 71-042A, 71-043, 71-047, and 71-052 are located on line 112W approximately 2200 feet west of the western tip of the Faro #1 orebody. Two holes are located on line 136W and both contain the continuing intercepts of anomalous Pb values but with no coinciding anomalous Cu or Zn values.

Three holes with continuing intercepts of anomalous metal content are located on line 160W. Analyses of samples from two of these show anomalous Pb within the drilled interval and one (Hole 71-065) contained anomalous Cu, Pb, and Zn in the top 30 feet when first drilled, but the anomalous values were not repeated when this hole was redrilled as 71-065A.

On the East Faro grid, the area southeast of grid line 64W, eight holes contained continuing intercepts of samples with anomalous metal content. Six of the eight holes with anomalous metal values are located along grid line 28W across the Faro #2 orebody. One hole, 71-086, is located on line 52W 4000S and one hole is located on line 4W 2000N. The five samples with more than two elements present in anomalous quantities are all spatially closely related to the Faro #2 orebody and may in large part be attributed to the presence of this suboutcropping orebody. At the present time, it has not been determined positively whether the migration of metals is due to mechanical transportation or solution and migration of ions, but mechanical transport is probably the primary mode of metal transport.

### BOB-DY-RICH Area

In the BOB-DY-RICH area, highly anomalous metal values, those greater than three times the arithmetic averages, were detected in samples from holes which clustered in the same area. The closely spaced holes which contained the anomalous metal contents were 71-001, 71-002, 71-003, 71-004, 71-005, 71-006, 71-026, 71-027, 71-028, 71-029, 71-030, 71-031, 71-032, 71-033. Of these holes, four (71-002, 71-003, 71-006, 71-028) contained both anomalous lead and zinc in the same samples.

On basis of metal content in overburden and bedrock samples, selected targets were drilled with deep rotary holes. Three holes on the BOB-DY-RICH claims were deepened to a maximum of 430 feet. One hole, 71-028, redrilled as 71-197, yielded anomalous metal values in bedrock. The combined Pb-Zn values increased from 1830 ppm at 130-140 feet near the top of the bedrock intercept to a maximum of 6000 ppm at 160-170 feet, and then gradually decreased to 1100 ppm at 400-405 feet at which depth drilling had been stopped. The other two deep drill holes in this area revealed no anomalous metal content in bedrock samples.

The bedrock geology was identified for all holes and all samples with anomalous metal content were examined for presence of sulfide mineralization. Base metal sulfides were not noted in the initial logging of samples from hole 71-197.

### SUN-TIE-GAL Area

In the SUN-TIE-GAL area an apparent clustering of holes with anomalous metal content was revealed along the western border of the Vangorda claim block and the possible western extensions of the Vangorda and Champ orebodies. The anomalous values in this area were two times the average metal content. If samples with more than three times the average metal content were compared no samples contain anomalous Cu, and only one hole, 71-172, on the SUN claim contains anomalous Pb in more than one sample. All samples in hole 71-034 contained anomalous zinc content. Samples from one hole, spatially closely related to the Firth orebody, contained anomalous zinc.

In the SUN-TIE-GAL area, no samples contained more than four times the arithmetic average of any of the metals analyzed.

### Conclusions Regarding the Overburden Geochemistry Drilling

The overburden drilling program was effective in outlining areas of known suboutcropping sulfide mineralization on the east Faro grid. Areas on anomalous metal content in bedrock with coinciding geophysical anomalies contained no massive mineralization on the west Faro grid when rotary drill holes were drilled to 400 feet.

In the SUN-TIE-GAL area, anomalous metal contents were detected in samples from various drill holes. None of these holes contained samples with metal values with similar abundance and distribution to those on the east Faro grid across the Faro #2 orebody or to values on the BOB-DY-RICH claims.

The use of overburden drilling for bedrock identification was of limited use and then only in selected areas. In most areas, sufficient outcrop was available to make a reasonable inference of rock contacts and distribution. Generally in areas of limited outcrop but shallow overburden the dozing of lines to drill sites usually exposed sufficient bedrock for geological mapping.

In areas of deep cover, the rotary drilling method provided an excellent method for sampling overburden. Analysis of overburden was an effective way to prospect for suboutcropping orebodies where bedrock is more than about 100 feet deep. In areas where overburden is shallower than this, a soil geochemical survey should indicate the presence of mineralization. This was revealed by the overburden survey over the Faro #2 orebody.

DIAMOND DRILLING - 1971

Eleven BQ size diamond drill holes, comprising 5203 feet of drilling of selected targets, were completed from October 20, 1971 to December 28, 1971. Nine of these drill holes were confined to the Faro claims to test possible extensions of known mineralization. One hole was located on the BILL claims tested gravity target near a geochemical-electromagnetic anomaly in an area of known disseminated minor sulfide mineralization. One hole on the SUN claims tested a gravity anomaly near a zone of geochemical lead-zinc anomalies which extend to the northwest from the Vangorda mineralized zone.

The diamond drilling on the Faro claims tested extensions of known zones of mineralization. Three holes, 71-204, 71-207, 71-211, were drilled on the north dipping limb of the Faro anticline to test geologic extensions of Faro 1 and Faro 3 orebodies. One hole, 71-209, tested the eastern and southern extensions of Faro #2 across the north fork of Rose Creek. Four holes, 71-210, 71-215, 71-216, 71-217, were drilled north of the Faro #2 orebody and east of the southeastern tip of the Faro #3 orebody. This drilling was designed to test the extensions of mineralization encountered previously in Dynasty's original rotary hole FRH-2. Hole 71-210 intercepted 10.5 feet of sulfides, averaging 2.9% Pb and 3.32% Zn. Three holes, 71-215, 71-216, 71-217, were then drilled to test extensions of mineralization in 71-210. Minor non-economic sulfide mineralization was encountered in these definition holes thus limiting the areal extent of the 71-210 sulfides to 1000 x 1400 feet east-west by north-south. Assuming an average thickness of 10 feet, on basis of sulfide intercepts in 71-210, and using a tonnage factor of 10 cubic feet per ton, a maximum of  $1.4 \times 10^6$  tons of sulfides might be expected in this area. Assuming sulfide extensions are continuous for half the distance between drill holes, approximately 700,000 tons of sulfides are indicated. One drill hole, 71-214, tested the possible sulfide mineralization underneath a strong soil geochemical anomaly in the "boneyard" at the minesite. This hole encountered calc-silicate rock with only traces of sulfide minerals.

On the BILL claims, one drill hole, 71-212, tested the mineralization in an area of a 0.3 milligal gravity anomaly, metal in soil anomaly and presence of minor disseminated sulfide mineralization in an area of airborne E-M anomalies. These E-M anomalies were connected with and are extensions of airborne E-M anomalies that are also spatially related to the Faro 1, 3, and 2 orebodies. Graphitic

schist with minor (about 3% estimated) pyrite mineralization was encountered in the top 160 feet of this hole. Biotite muscovite schist with trace sulfide, mainly pyrite and minor pyrrhotite, was encountered in the rest of the hole.

On the SUN claims, one drill hole, 71-208, tested a gravity anomaly that was spatially related to a major elongate Pb-Zn in soil geochemical anomaly which, further to the southeast, partially overlies the Vangorda orebody. This drilling encountered amphibolite at a depth of 674 feet. This may have been a source of the gravity anomaly.

The individual drill holes depth, location, reason for drilling, and results are shown on the following table.

Diamond  
Drill  
Hole

Location

Depth

Reason for Drilling

Results

Diamond Drill Hole	Location	Depth	Reason for Drilling	Results
71-204B	56W 2NBL Faro Grid	126 ft.	Overburden geochem	Anvil batholith
71-207	83W 63N Faro Grid	678 ft.	Geologic projection of Faro #1, gravity anomaly	Started in calc silicate, then biotite schist, graphitic schist 250-259. Calc silicate 490-612. Bottomed in Anvil batholith.
71-208	112W 44N SUN Grid	891 ft.	Regional soil geochem, gravity, sulfides in SRH-4	Started in amphibolite, graphitic phyllite 90-530. Chl. ser. schist 530-674. Greenstone at 674 to 891.
71-209	- Faro Grid	600 ft.	Gravity anomaly, geologic projections of Faro #2	Minor sulfides (~1%) in sericite schist at 226-236. Bottomed in biotite ser. schist.
71-210	3W CBL Faro Grid	502 ft.	Projection of FRH-2 sulfides on S <sub>2</sub>	10.5 ft. sulfides in 18-29.5 feet, ingraphitic qtzschist. Bottomed in bio. seric. schist. 6.2% Pb-Zn
71-211	52W 28N Faro Grid	501 ft.	Geologic projection of Faro 1 and 3 to N limb of Faro anticline	Started in bio-ser schist - several breccia gouge zones. Bottomed in Anvil batholith.
71-212	- BILL claim	500 ft.	Geochem, gravity, E-M connects this with Faro #2 zone.	Started in quartzite, graphitic phyllite w/~3% pyrite 43-48. Bottomed in biotite sericite schist.
71-213	71-028 Site DY claims		Bedrock geochem, gravity anomaly	To be Drilled.
71-214	(8W 18S) Boneyard Faro Grid	300 ft.	Geochem anomaly	Calc silicate, no sulfides in bedrock
71-215	27W 2S Faro Grid	278 ft.	Zone between FRH-2 and 71-210 sulfides	Started in biotite sericite schist. Minor sulfides (0.25% Pb, 0.5% Zn) 31-44' W qtz ser. schist & graphitic schist. Bottomed in bio-ser schist.
71-216	34W 3N Faro Grid	300 ft.	Detail 71-210 sulfides to E., gravity anomaly	Massive qtz sulfide fragments w/seric mud in overburden and bedrock interface (0.3% Pb, 0.25% Zn). Bottomed in biotite sericite schist.

Diamond Drill Hole	<u>Location</u>	<u>Depth</u>	<u>Reason for Drilling</u>	<u>Results</u>
71-217	34W 9S Faro Grid	483 ft.	Detail 71-210 sulfides to S. towards Faro #2, soil geochem anomaly	Started seric. bio. schist. Minor sulfides (~ 3% py 80' - 99'). Bottomed in biotite muscovite schist.

ASSESSMENT STATUS OF CLAIMS

The assessment status of Anvil Mining Corporation's and Pelly River Mines' claims is depicted on Figure 28. The expiration dates of the claims and claim groups is colour coded in the following manner:

	<u>Expiry Year</u>
Red	1972
Green	1973
Blue	1974
Black	1975 and later

These dates represent the years to which time extensions have been granted or requested but not yet granted.

It is of prime interest to identify claims on which work will be required in 1972. Inspection of Figure 28 shows that none of the claims in the area of contiguous claim blocks northwest of Blind Creek require assessment work in 1972. In the area southeast of Blind Creek, assessment work will be required for all or part of the following claims (together they are later referred to as the Swim Lake group):

<u>Claim Number</u>	<u>Number of Claims</u>
CAROL	3
DEA	10
DY	8
KAY	17
LEA	16
PEA	27
RAM	28
SEA	70
TED	22

Claims outside the main contiguous claim blocks that have a 1972 expiry are the RAM claims, located on Anvil Creek approximately eight miles north of the minesite and the TED group, located near the confluence of Teddy Creek and the Tay River, located approximately twenty-eight miles northeast of the minesite.

The dates of expiry for claims in 1972 are:

RAM Claims	May 30, 1972
Swim Lakes Area Claims (CAROL, DEA, DY, etc.)	May 1, 1972
TED Claims	October 21, 1972

SUMMARY OF 1971 EXPLORATION BUDGET

Of \$478,236 budgeted for 1971 exploration program, \$468,745.62 had been spent by December 31, 1971. One item, consisting of base for regional geologic mapping, is still to be charged to the 1971 budget. The estimated cost of these maps is \$5,000.

The expenditures of the 1971 budget, as known on January 15, 1972, are itemized on the following page. No major charges, other than the base maps, are to be included in the final account.

	<u>Acct.</u> <u>No.</u>	<u>Budgeted</u>	<u>Expenditures</u>	<u>% To</u> <u>PRM</u>	<u>Anvil</u> <u>Share</u>	<u>Pelly</u> <u>Share</u>
borne Survey	00	20,000	-	-	-	-
Contract Gravity	10	1,875	3,240	-	3,240	-
<b>Drilling</b>						
Contract Work	20	261,375	279,202	26	206,609	72,593
Supplies	22	983	1,811	26	1,340	471
Sample Analysis	28	4,414	1,595	26	1,181	415
Consulting	30	4,160	4,937	20	3,950	987
Outside Services	40	6,718	5,413	26	4,005	1,407
<b>Soil Sampling</b>						
Labour	50	6,750	4,330	20	3,464	866
Materials	52	300	1,878	20	1,503	376
Analysis	58	21,640	12,524	20	10,019	2,505
<b>Equipment Costs</b>						
Labour - Operating	60	( )	7,022	26	5,197	1,826
- Repair	61	( 43,107 )	5,916	26	4,378	1,538
Supplies - Oper.	62	( )	3,275	26	2,424	852
- Repair	66	( )	5,015	26	3,711	1,304
Fuel	64	15,953	11,677	26	8,641	3,036
<b>mp Costs</b>						
Labour	70	8,210	14,127	26	10,454	3,673
Supplies	72	17,018	13,428	26	9,937	3,491
<b>Geology</b>						
Labour & Supplies	80	21,365	22,196	12	19,532	2,663
<b>Supervision</b>						
Labour	90	16,716	13,498	26	9,989	3,510
Supplies	92	1,105	3,558	26	2,633	925
Diamond Drilling		42,500	49,191	10	44,272	4,919
Accrual					<u>3,950</u>	<u>733</u>
			<u>\$ 463,833</u>		<u>\$ 360,429</u>	<u>\$ 108,090</u>

OUTLINE OF THE 1972 EXPLORATION PROGRAM

The first goal of the 1972 exploration program will be to continue and complete the 1971 program of acquiring surface geochemical and geological information. The second goal of the 1972 exploration program will be to evaluate the existence of massive sulfide mineralization at various depths below the entire claim surface area. In addition to the main programs, work will be done to evaluate specific anomalies and zones of interest which became apparent during the 1971 exploration.

General programs for the surface evaluation will include a soil geochemical survey to extend the 1971 program from Blind Creek to the southeast extensions of the Anvil claim groups.

The soil sampling during 1971 readily indicated areas of known sulfide mineralization. The soil orientation survey showed that suboutcropping ore at a depth of 60 feet was readily detected and delineated by a soil survey. Sulfides suboutcropping at depths greater than 60 feet should also be detectable by this method.

The second phase of the surface evaluation program will be the completion of the geological mapping program. Basic goals of this program, in addition to outlining the regional structure and "stratigraphy", will be to determine the position of the Faro, Vangorda, Swim, Champ, Firth mineralized zones within the "stratigraphic" column. As is obvious from the 1971 program, the host rocks at the Faro orebodies are different from the host rocks at the Vangorda, Champ and Firth orebodies. Also obvious and of significance is the spatial relationship of the known mineralized zones at Faro, Vangorda, Swim and Firth with graphite bearing, rock units, as outlined by the original airborne E-M survey. All of the known orebodies show the above relationship of sulfide zones spatially related to graphitic zones.

Following the surface evaluation of the claim groups, the emphasis of the program will shift to evaluate the subsurface. The first subsurface zone of interest is the overburden in which the metal content can be investigated by geochemical methods. Because of the reported deep overburden in the Swim Lakes area, a method of rotary drilling and overburden and bedrock sampling, similar to that done in 1971, may be proposed for selected areas of interest that may be indicated following the surface work. The second phase is evaluation of possible zones of mineralization in bedrock. The geochemical orientation program showed that bedrock geochemical halos do not surround mineralized zones, and therefore these would not be detected by geochemical soil surveys. Other methods that might reveal massive

sulfide zones enveloped in bedrock have to be based on geophysical exploration concepts. For example, sulfide mineralization in the Anvil range is known to be spatially related to zones of graphite bearing rocks. Therefore, areas of anomalous conductors located by the airborne E-M survey should be further investigated by either electrical or gravity methods to locate possible concentrations of high conductivity and high density sulfide masses. Target selection would, of necessity, involve examining areas in which "favourable rock units" are known to exist and areas of interest that can be outlined by geophysical reconnaissance methods and geological projections.

In addition to the general program outlined above, more detailed work will be required to follow up the results of the 1971 exploration. This work includes:

1. Evaluation of DY-BOB-RICH area of bedrock geochemical anomalies by diamond drilling.
2. Evaluation of SUN-TIE-GAL area soil geochemical anomaly.
3. Evaluation of BILL claim geochemical anomaly.
4. Evaluation of the airborne E-M and magnetic anomalies northwest of the water storage dam.
5. Evaluation of RAM, TED, and CROWN claims. The RAM and TED claims have sufficient data for possible drilling. Field work is required on the CROWN claim.

Further work on Anvil and Pelly River Mines will be the completion of assessment requirements for claims with 1972 expiry dates.

The budget for the exploration in 1972 is \$200,000 from Anvil Mining Corporation Limited. Funds in addition to the basic budget will require from Pelly River Mines approximately \$5000 for expenses in geological mapping of Pelly River Mines' claims.

The 1972 exploration program will require personnel in addition to the present staff. The present staff includes two geologists, one draftsman, and one drilling supervisor. The additional personnel requirements envisaged are:

1. PhD candidate to help surface mapping
2. Geology student - geology technician to run soil sampling program and other routine work.
3. Soil sampler.
4. Surveyor and assistant to tie together all existing grids, the 1971 rotary drill holes and other work as required.

APPENDIX I

GEOCHEMICAL ORIENTATION STUDY  
IN THE ANVIL MINING DISTRICT  
YUKON TERRITORY

prepared by  
Uldis Jansons

for

ANVIL MINING CORPORATION LIMITED

FARO, YUKON TERRITORY

December 17, 1971

## APPENDIX I

### Geochemistry - Soils and Bedrock

#### Soil Geochemistry

##### Orientation Surveys

Sampling and Analytical Precision

Sample Material Evaluation

Soil Orientation - Metal Content

Soil Horizon

Metals in Till

Metals in Moss

Metals in Volcanic Ash

Evaluation of Mercury in Soils for Geochemical Prospecting

#### Overburden-Bedrock Geochemistry

Average Metal Content in Overburden and Bedrock

Average Metal Content in Various Rock Types

Overburden Geochemical Orientation

Comparison of Metal in Soil and Overburden

Bedrock Orientation Survey

Conclusions

## GEOCHEMISTRY - SOILS AND BEDROCK

Soil and bedrock materials were sampled during the 1971 exploration program. The following is an evaluation of orientation surveys for both the soil and bedrock materials.

### Soil Geochemistry

Soil samples were collected over the Anvil claims on a grid pattern with sampling stations located at 200 foot intervals on lines spaced 1200 feet apart. The "B" horizon was selected to be analyzed for total Cu, Pb, Zn and Hg content in the -80 mesh fractions using  $\text{HClO}_4$  extraction. An orientation survey was conducted about half way through the soil sampling program to determine if the proper elements were being analyzed. The sampling and analytical work was by Barringer Research Ltd. The results of that orientation survey are outlined below.

### Orientation Surveys

Three orientation surveys were conducted. These surveys were to evaluate a) sampling and analytical precision; b) metal in various materials at a sample site; and c) evaluation of elements to be analyzed.

### Sampling and Analytical Precision

The sampling precision was determined by taking five samples within a fifty foot radius of a sample station. The analytical precision was determined by splitting one sample into five portions and analyzing each portion separately. The sample station selected for these experiments was 2800W 4S on the soil sampling grid. The results are shown below.

Multiple Samples:

<u>Sample Station</u>	<u>Sample</u>	<u>Cu (ppm)</u>	<u>Pb (ppm)</u>	<u>Zn (ppm)</u>	<u>Cd</u>	<u>Hg</u>
2800W 4S	A	13	30	58		
2800W 4S	B	13	32	55		
2800W 4S	C	12	30	57		
2800W 4S	D	14	30	68		
2800W 4S	E	12	28	62		
		Avg. 13	Avg. 30	Avg. 60		

Multiple Analyses of One Sample:

2800W 4S	E1	12	28	62		
2800W 4S	E2	13	28	61		
2800W 4S	E3	15	32	69		
2800W 4S	E4	20	34	68		
2800W 4S	E5	13	28	69		
		Avg. 15	Avg. 30	Avg. 66		

Visual inspection of the above data suggests nearly identical results for the five samples taken within the fifty foot radius of a sample station. More variation was shown in the sample splits than in the multiple samples. In general, the average metal content in the samples did not vary more than 10% from the arithmetic mean.

Sample Material Evaluation

An orientation program was conducted over the Faro #2 orebody along line 28W. The spatial relation of the samples to Faro #2 orebody are shown on Figure I. Materials collected at these sample stations are soil, ash, till, and moss. The individual sample descriptions below are taken from the preliminary data submitted by Barringer Research Ltd.

"The soil profile development in the Faro area is virtually nil. Much of the area is underlain by a compact till (generally a ground morrain) while the valleys are filled with alluvium. The till is irregularly overlain by a white volcanic ash and everywhere overlain by an organic layer.

Details of the individual horizons samples are as follows: Moss - this is largely living matter, principally moss but also with roots of higher plants and some undecomposed leaves etc. The mineral content is quite low. This layer generally varies between 2 and 4 inches thick and is always present.

A<sub>1</sub>\* - this is decomposed organic matter. Although very high in organics, there is no recognizable plant material such as leaves, moss, etc. except for roots penetrating this horizon from higher up. This horizon is generally present, and grades into the upper moss layer. In some cases the mineral content is high but generally not. This layer generally varies between ½ and 3 inches.

Ash - this layer is of volcanic origin. It occurs below the A<sub>1</sub>, and above the till and has sharp contact with both. The ash layer is only irregularly present and varies between 0 and 6 inches.

Till - the till is generally a very compact mixture of clay/silt and gravel. The coarser fragments are usually angular to sub-angular and this till is probably of fairly local origin. In the order of several 100 feet, in the majority of cases. In some areas however, although still compact the till shows signs of rusting and most of the fragments are rounded. This material has undergone some water transportation and is transported a greater distance than the more angular till.

The till, where it can be observed in cross-section, shows a rough horizontal banding. These bands undoubtedly are of different local origin and this will be reflected in the geochemistry."

\* A<sub>1</sub> is used here for the same material called "B" soil in other Anvil reports. The terms have been used by different writers but are interchangeable.

Materials Sampled:

<u>Sample No.</u>	<u>Depth In Inches</u>	<u>Type</u>	<u>Organic Content</u>	<u>Color</u>	<u>Comments</u>
#1 AM 1	0-2	Moss	Very high	Black	Living matter, largely moss & undecomposed plant material.
AM 2	0-2	Al	High	Black	Decomposed plant litter & some mineral matter.
AM 3	4-8	Till	-	Brown	Compact, angular clay-grave
AM 4					" " " "
AM 5	9-12	Till	-	Brown	
AM 6					
#2 AM 7	0-2	Moss	Very high	Black	As for AM 1
AM 8	2-8	Al	High	Black	As for AM 2
AM 9	8-16	Till	-	Brown	As for AM 3
#3 AM 10	0-4	Moss	Very high	Black	As for AM 1
AM 11	4-12	Al	High	Black	As for AM 2
AM 12					
13	12-18	Till	-	Darkbrown	As for AM 3
14					
#4 AM 15	0-7	Moss	Very high	Red brown	As for AM 1
AM 22	7-8	Al	Low	Brown	As for AM 2 but less well developed, sandy
AM 16	8-12	Ash	-	White	Volcanic ash
AM 17	12-16	Till	-	Brown/blk	As for AM 3
#5	(collected from stream cutting)				
AM 18	0-5	Moss	Very high	Yellow/red	As for AM 1
AM 19	5-12	Al/B	Moderate	Brown	As for AM 2 but high mineral content, silts
AM 20	12-24	Till	-	Grey	As for AM 3
AM 21	24-36	Till	Low	Black/grey	Till band containing some organic matter.
#6 AM 23	0-6	Moss	Very high	Black	As for AM 1
AM 24	2-3	Al	High	Black	As for AM 2
AM 25	3-6	Ash	-	White	Volcanic Ash
AM 26	6-12	Al/B	-	Dark brown	As for AM 2, but high mineral content, sandy
AM 27					
AM 28	12-18	Till	-	Brown	As for AM 3
AM 29					

<u>Sample No.</u>	<u>Depth In Inches</u>	<u>Type</u>	<u>Organic Content</u>	<u>Color</u>	<u>Comments</u>	
#7	(collected from stream cutting)					
AM 30	0-2	Moss	Very high	Black	As for AM 1	
AM 31	2-6	Al	High	Black	As for AM 2	
AM 32	6-18	Till		Grey	As for AM 3	
AM 33	72-96	Till	-	Red/Brown	As for AM 3 but limonite rich.	
#8	AM 34	0-2	Moss	Very high	Black	As for AM 1
	AM 35	2-6	Al	High	Dark brown	As for AM 2
	AM 36	6-18	Till	-	Light brown	Impact, rounded, sorted, sandy
	AM 37					
	AM 38					
#9	AM 40	0-2	Moss	Very high	Black	As for AM 1
	AM 41	2-4	Al	High	Black	As for AM 2
	AM 42	4-8	Ash	-	White	Volcanic Ash
	AM 43	8-16	Till	-	Red brown	As for AM 36
#10	AM 44	0-2	Moss	Very high	Black	As for AM 1
	AM 45	2-3	Al	Low	Brown	As for AM 2 but high mineral content, sandy.
	AM 46					
	AM 47	3-12	Till	-	Dark brown	As for AM 36
	AM 48					
#11	AM 49	0-2	Moss	Very high	Black	As for AM 1
	AM 50	2-3	Al	Low	Brown	As for AM 2 but high mineral content, silty
	AM 51	3-15	Till	-	Brown	As for AM 36

### Soil Orientation - Metal Content

The soil orientation survey along line 28W over the Faro #2 ore zone involved collecting soil, moss, ash, and till materials for chemical analysis at eleven sample stations. This material was analyzed for total Ag, As, Ba, Cu, F<sup>-</sup>, Hg, Mn, Pb, Sb, Te, and Zn content.

A<sub>1</sub> Soil Horizon - Eleven elements were analyzed in A<sub>1</sub> horizon soils collected across the Faro #2 orebody along grid line 28W to determine which could be related to an underlying suboutcropping sulfide mass. The metal values along this line are plotted in profile form in Figure 1 showing spatial relations to the orebody.

Readily recognizable anomalies are shown by As, Cu, Hg, Pb, Zn, and possibly Mn. Arsenic and mercury show a broad dispersion of values around the orebodies. The Hg anomaly appears to have migrated down slope from the known mineralized zone. Poorly defined or no anomalies are shown by Ag, Ba, F<sup>-</sup>.

Two separate anomalies - one over the Center Base Line and one over Faro #2 are identified by Pb, Zn, and possibly Hg. Arsenic values are lacking (insufficient samples for analysis) in the areas between these peaks and no conclusions can be drawn regarding the dispersion of As.

The factors of increases in metal values are seen from background to maximum anomalous values over ore.

As	$\frac{17}{2}$	=	8.5	Mn	$\frac{1700}{78}$	=	21.8
Cu	$\frac{140}{14}$	=	10	Pb	$\frac{140}{16}$	=	8.75
Hg	$\frac{4535}{189}$	=	22.8	Zn	$\frac{1650}{42}$	=	39.3

Pb and Zn yielded the highest values in samples spatially closely related to Faro #2. The Mn and Cu in soils show anomalous concentrations in soils in an area between the anomalous Pb and Zn values. The high Mn value at this location coincides best with the anomalous Hg values, but it is less extensive areally than the Hg anomaly.

Metals in Till - The abundance and variation of the Ag, As, Ba, Cd, Cu, F<sup>-</sup>, Hg, Mn, Pb, Sb, and Zn content in till along grid line 28W over the Faro #2 orebody was investigated. The metal values along this line are plotted on Figure 2 showing spatial relationship to the orebody.

Readily recognizable anomalies are shown by As, Cd, Cu, F<sup>-</sup>, Hg, Pb, and Zn. Poorly defined or no anomalous content is shown by Ag, Ba, Mn, and Sb. Two zones of anomalous element content are revealed on Figure 2 one spatially closely related to the Faro #2 orebody and one located near the Center Base Line. The metal abundances are lower in samples related to the Faro #2 orebody than those near the Center Base Line.

The variation of the metal content with depth of sampling was investigated. Two stations were sampled at different depths. The set of samples taken at Station 5 approximately 200 feet south of the Center Base Line, was taken at the depths of 12-24 inches and 24-36 inches. The second sample taken at Station 7 over the Faro #2 orebody was collected in the intervals 6-18 inches and 72-96 inches. The results of analyses of samples taken is given below (all values are in parts per million except Hg, which is given in parts per billion, and organic carbon which is given in percent).

<u>#5</u>	<u>Ag</u>	<u>As</u>	<u>Ba</u>	<u>C(%)</u>	<u>Cd</u>	<u>Cu</u>	<u>F<sup>-</sup></u>	<u>Hg</u>	<u>Mn</u>	<u>Pb</u>	<u>Sb</u>	<u>Zn</u>
12"-24"	1.1	25	390	1.68	3	130	924	135	1400	400	1	1400
24"-36"	0.2	25	360	7.87	11	300	408	3731	3350	240	1	3350
<u>#7</u>												
6"-18"	0.2	10	200	0.68	4	48	860	217	280	74	1	1050
72"-96"	1.4	12	250	0.31	6	170	288	718	330	158	1	2350

Metal Content in Moss - The abundance and variation of As, Cu, Hg, Mn, Pb, Te, and Zn in moss sampled along line 28W over the Faro #2 orebody was determined. The metal values along the sample line are shown in profile form in Figure 3. All elements analyzed, except Te, were present in anomalous amounts in samples spatially closely related to suboutcropping sulfide mineralization.

The greatest increase in values near ore was shown for Hg, Mn, and Pb, followed by the group As, Cu, Zn. Te and Sb showed no readily visible variations.

The following table shows the maximum and minimum metal values and the factor of increase in metal content from background to anomalous values.

	<u>Hg</u>	<u>As</u>	<u>Mn</u>	<u>Zn</u>	<u>Pb</u>	<u>Cu</u>	<u>Te</u>
Maximum	5838	22	6800	3100	2400	215	1
Minimum	119	1	34	29	10	10	1
Increase	49.2	22	200	107	240	21.5	-

Metals in Volcanic Ash - The metal content in three volcanic ash horizon samples along line 28W over the Faro #2 orebody was determined. Plotting of the analytical results in profile form along the sample line does not provide sufficient data to evaluate the spatial relationship of metal abundances in volcanic ash to the orebody.

Visual inspection of the metal abundances indicates that the volcanic ash is generally depleted in metal relative to till and A<sub>1</sub> soil. The differences are not systematic. For example, Cu, Pb, and Zn are 2 to 76 times higher, Mn is about 15 times higher, Ag is 2 times higher, and Ba is 3 to 6 times higher in till and A<sub>1</sub> soil than in the volcanic ash.

A detailed test of the use of the volcanic ash layer for mineral soil sampling in the Vangorda Creek area was conducted by J.A.C. Fortescue of the Geological Survey of Canada. He concluded that metals in the ash layer are generally lower than those in the "B" soil horizon, but anomalous values found in one material are almost identical to those found in the other. Fortescue's report and analytical results are shown below.

"During a brief visit to the Vangorda Creek area of the Yukon during August 1966, the writer collected fifteen samples of volcanic ash and fifteen samples of B horizon material from each of two sets of soil pits, one located over the Faro No. 1 orebody, and the other over Faro No. 3. These mineral soils were taken to Ottawa, oven dried, sieved in a stainless steel sieve and the minus 80 mesh material analyzed for total zinc, lead, copper and nickel. The metals were extracted from the samples by a hot HF/HClO<sub>4</sub> extraction and the copper, lead and zinc were determined by a method due to Gilbert (1959) and the nickel by a method due to Stanton and Coope (1962).

The analytical results are shown on Table 1. The sampling was carried out so that high values and low values were obtained in each set of samples. The results for samples taken in the ash layer are generally lower than those taken in the underlying B horizon, but from the prospecting point of view, anomalous values found in one material are almost identical with those found in the other. For this reason, it is believed that in the vicinity of Faro No. 1 and Faro No. 3, either the volcanic ash or the B horizon of the soil will give useful results. The advantages of using the ash layer include 1) it is easily recognized by unskilled samplers, 2) the sample pits need not be so deep as those for the collection of the B horizon, and possibly 3) if spectrochemical analysis is used on samples, the volcanic ash layer is a relatively uniform matrix."

TABLE I

Comparison of Metal Content in Volcanic Ash and "B" Soil Horizons  
Along Grid Lines 36 West and 80 West of the Faro Grid

(from J. A. C. Fortescue)

A = Ash Samples

B = "B" Soil Horizon Samples

STAT- ION	<u>LINE 36 W</u>						<u>LINE 80 W</u>						
	(Over Faro No. 3)						(Over Faro No. 1)						
	ppm Cu		ppm Pb		ppm Zn		STAT- ION	ppm Cu		ppm Pb		ppm Zn	
A	B	A	B	A	B	A		B	A	B	A	B	
19 N	52	32	45	35	130	130	21 N	36	32	5	15	70	110
17 N	36	36	40	30	160	130	20 N	28	36	5	5	70	120
15 N	48	32	35	25	120	170	19 N	4	16	5	35	60	170
13 N	48	56	40	50	130	180	18 N	28	24	5	90	70	230
11 N	48	44	50	90	170	170	17 N	28	20	140	140	170	340
9 N	44	44	120	140	180	180	15 N	24	20	50	140	180	260
8 N	44	72	240	700	180	240	14 N	48	28	100	230	580	460
7 N	52	48	240	200	260	460	13 N	32	20	65	140	170	260
5 N	52	48	280	220	280	270	12 N	28	28	60	50	220	220
3 N	48	40	270	180	340	290	11 N	32	34	5	40	70	170
2 N	64	68	460	220	440	600							
1 N	52	120	70	45	260	3400	10 N	28	32	5	70	70	270
1 S	16	20	5	30	60	170	9 N	28	8	5	20	40	140
3 S	12	20	5	20	70	150	8 N	28	32	55	55	120	240
5 S	24	24	15	80	40	180	7 N	52	40	120	100	220	240
							6 N	68	36	45	45	170	180

Evaluation of Mercury for Geochemical Prospecting in the Anvil Range

The use of mercury in exploration was investigated in detail in the orientation survey. Materials were sampled in detail and the mercury content in soils and moss was examined for abundance and relations.

Various methods of sample drying were compared to determine if the temperature of drying affected the final mercury content in final analysis.

The various experiments are summarized below.

Comparison of Mercury Content in Soil and Moss

	<u>Organic Soil</u> (ppb Hg)	<u>Moss</u> (ppb Hg)	<u>Ratio</u> { $\frac{\text{Moss}}{\text{Org. Soil}}$ }
# 1	112	219	1.95
# 2	25	1121	15.0
# 3	129	153	1.185
# 4	64	119	1.86
# 5	228	261	1.14
# 6	540	135	.25
# 7	457	5838	12.79
# 8	56	177	3.17
# 9	170	177	1.04
# 10	174	146	.84
# 11	<u>66</u>	<u>219</u>	<u>3.32</u>

Above information shows that the mercury content in moss is generally higher than in organic soils. The ratios of the mercury in moss to mercury in soil were determined also to see if a systematic difference could be determined. The ratios show again that the mercury content in moss is higher than in soils, but the difference is only constant for 4 of the 11 samples and the spreads in the ratios range from 0.25 to 15.0. The mercury content of soils dried at room temperature, at low oven heat, and at high oven heat are compared below.

Comparison of mercury content in soils - Material dried at Room Temperature (R), Low Temperature (L), High Temperature (H):

	<u>R</u>	<u>L</u>	<u>H</u>		<u>RATIOS</u>		
1) Sample Number	# 3	# 5	# 6				
ppb Hg	15	57	103				
2) Sample Number	#27	#28	#29				
ppb Hg	24	68	83				
					<u>L/R</u>	<u>R/H</u>	<u>L/H</u>
3) Sample Number	#46	#47	#48	1)	.263	.146	.55
ppb Hg	100	98	80	2)	1.66	1.92	1.15
				3)	.35	.29	.82
4) Sample Number	#11	#13	#14	4)	.53	.61	1.14
ppb Hg	362	218	189	5)	1.02	1.25	1.23
5) Sample Number	#36	#37	#38				
ppb Hg	52	98	86				

Visual inspection of the analytical results shows poor precision in the mercury results, especially between the room temperature and oven dried materials. Better precision is obtained between the high and low temperature oven dried material. Note that most of the oven dried materials showed higher mercury content than the room dried material.

### Overburden-Bedrock Geochemistry

The metal content of overburden, bedrock material, and the metal content of the different rock types was determined. The metal content in holes along line 28W across the Faro #2 orebody was used as an orientation study to determine metal abundances and their spatial relations to mineralization. The metal values in these holes are shown on Figure 4.

#### Average Metal Content in Overburden and Bedrock

The average total metal content was determined in overburden and rock chip cuttings obtained by rotary drilling. The analysed samples represented 10 foot depth intervals. Rock samples were not initially separated into types and therefore the following analyses represent an overall average metal content of rocks.

	<u>Overburden</u>	<u>Bedrock</u>
Cu (ppm)	33	33
Hg (ppm)	77	52
Pb (ppm)	44	44
Zn (ppm)	133	133

No real differences in metal content (except possibly Hg) were distinguished between overburden and bedrock.

#### Average Metal Content in Various Rock Types

The average metal content in various rock types, present within the Anvil claim boundaries, was determined to see if a correlation could be made with the metal content in bedrock and the overlying soil. The chemical results of rotary drilling rock chip sample analyses were used. The rock types encountered in drilling were identified visually. The average metal content in various rock types calculated regardless of rock type is 33 ppm Cu, 52 ppm Hg, 44 ppm Pb, and 133 ppm Zn.

The average metal content of the specific rock types along with the number of samples averaged is shown on the following table.

Average Metal in Rock Types

<u>Rock</u>	<u>Pb</u> <u>ppm</u>	<u>Zn</u> <u>ppm</u>	<u>Cu</u> <u>ppm</u>	<u>Hg</u> <u>ppm</u>	<u>Cd</u> <u>ppm</u>
Calc Silicate					
$\bar{x}$	64	123	47	100	
n =	(211)	(203)	(200)	(104)	
Greenstone					
$\bar{x}$ =	41	115	31		
n =	2	2	2		
Felsites & Granites					
$\bar{x}$ =	56	96	31	55	2
n =	7	7	7	3	4
Graphitic Phyllites & Schists					
$\bar{x}$ =	40	118	40		4.2
n =	8	7	7		5
Quartz Mica Schists					
$\bar{x}$ =	39	101	42	29	3
n =	51	51	51	31	3
Chlorite Sericite Phyllites					
$\bar{x}$ =	43	110	50	118	2.2
n =	294	293	320	74	8

$\bar{x}$  = arithmetic average

n = number of samples

The average metal content, when compared, shows only a small difference between the various rock types. The range of values and a list of individual values for a specific metal in rocks is:

<u>Element</u>	<u>Range (ppm)</u>	<u>Values (averages for specific rock types)</u>
Pb	39-64	39, 40, 41, 43, 56, 64
Zn	96-123	96, 101, 110, 115, 118, 123
Cu	31-50	31, 31, 40, 42, 47, 50
Hg	29-118	29, 55, 100, 118

#### Overburden Geochemical Orientation

An orientation survey was performed to determine the metal distribution from a suboutcropping orebody into overlying glacial (?) overburden material. Five rotary holes were drilled on 1000 foot stations along line 28 W over the Faro #2 orebody. The distribution of these holes and their spatial relationship to the Faro #2 orebody are shown on Figure 4. Ten foot sample intervals were analysed for the total Cu, Hg, Pb, and Zn content. The Cu, Pb, and Zn distribution in these samples is shown on Figure 4. Visual examination of the chemical data shows values in drill hole 71-072, which penetrated the ore body, decreasing from 790 ppm Cu to 77 ppm Cu, 5800 ppm Pb to 94 ppm Pb, and from 41500 ppm Zn to 960 ppm Zn over a 60 foot vertical interval. The metal content in rotary drill hole 71-071, located 1000 feet uphill from 71-072 and the Faro #2 orebody, showed apparently random scattered intercepts of anomalous metal content.

The metal content in rotary hole 71-073 located approximately 500 feet past known extensions of the Faro #2 orebody suggests mechanical downslope transport. Highest metal values, especially of Pb and Zn, are found in the upper samples within the drill hole. However, all samples yielded highly anomalous metal contents. Hole 71-074, approximately 1500 feet downslope from the margins of the known orebody, still yielded anomalous metal contents but the values have decreased by a factor of 10 over a 1000 foot distance from hole 71-073. Highest Pb and Zn values again in hole 71-074 are located in the upper samples.

Comparison of Metal Content in Soil and Underlying Material

The metal content in the "B" horizon soil is compared with the metal in the underlying overburden material. A general comparison can be made first by using the average metal contents of soil and overburden. Then a comparison can be made with samples collected over the Faro # 2 orebody.

The average metal content of "B" horizon soils can be compared with the average metal content in overburden. The average metal contents in the two materials are:

	<u>Soil</u>	<u>Overburden</u>
Cu (ppm)	29	33
Pb (ppm)	33	44
Zn (ppm)	84	133
Hg (ppm)	--	77

The averaged values shown above indicate that the "B" horizons are not enriched in the metal content in the areas thought to be unmineralized. Therefore, the presence of zones of anomalous metal content in soil should be of interest for follow-up investigation.

Data are available for comparing the metal content in soils and the directly underlying overburden over a suboutcropping mineralized zone.

The data across the Faro # 2 orebody are listed below for comparison. The data are presented in profile form on Figure 4. The ratios of the metal values in soils are also calculated to see if a systematic difference is present.

<u>Location</u>		<u>Cu (ppm)</u>	<u>Pb (ppm)</u>	<u>Zn (ppm)</u>
71-069	Overburden	100	48	190
	Soil	80	40	270
	Ratio $\frac{O/B}{S}$	1.25	1.2	0.7
71-070	Overburden	470	60	710
	Soil	70	18	500
	Ratio $\frac{O/B}{S}$	6.72	3.3	1.42
71-071	Overburden	400	54	230
	Soil	15	110	600
	Ratio $\frac{O/B}{S}$	26.7	.49	.38
71-072	Overburden	77	94	960
	Soil	30	220	2600
	Ratio $\frac{O/B}{S}$	2.57	.43	.37
71-073	Overburden	440	5200	26400
	Soil	15	32	125
	Ratio $\frac{O/B}{S}$	29.3	162	211

The following generalizations can be made about the metal content in overburden and soil over a known mineralized zone:

- 1) The copper content is higher in the overburden material than in the overlying soil.

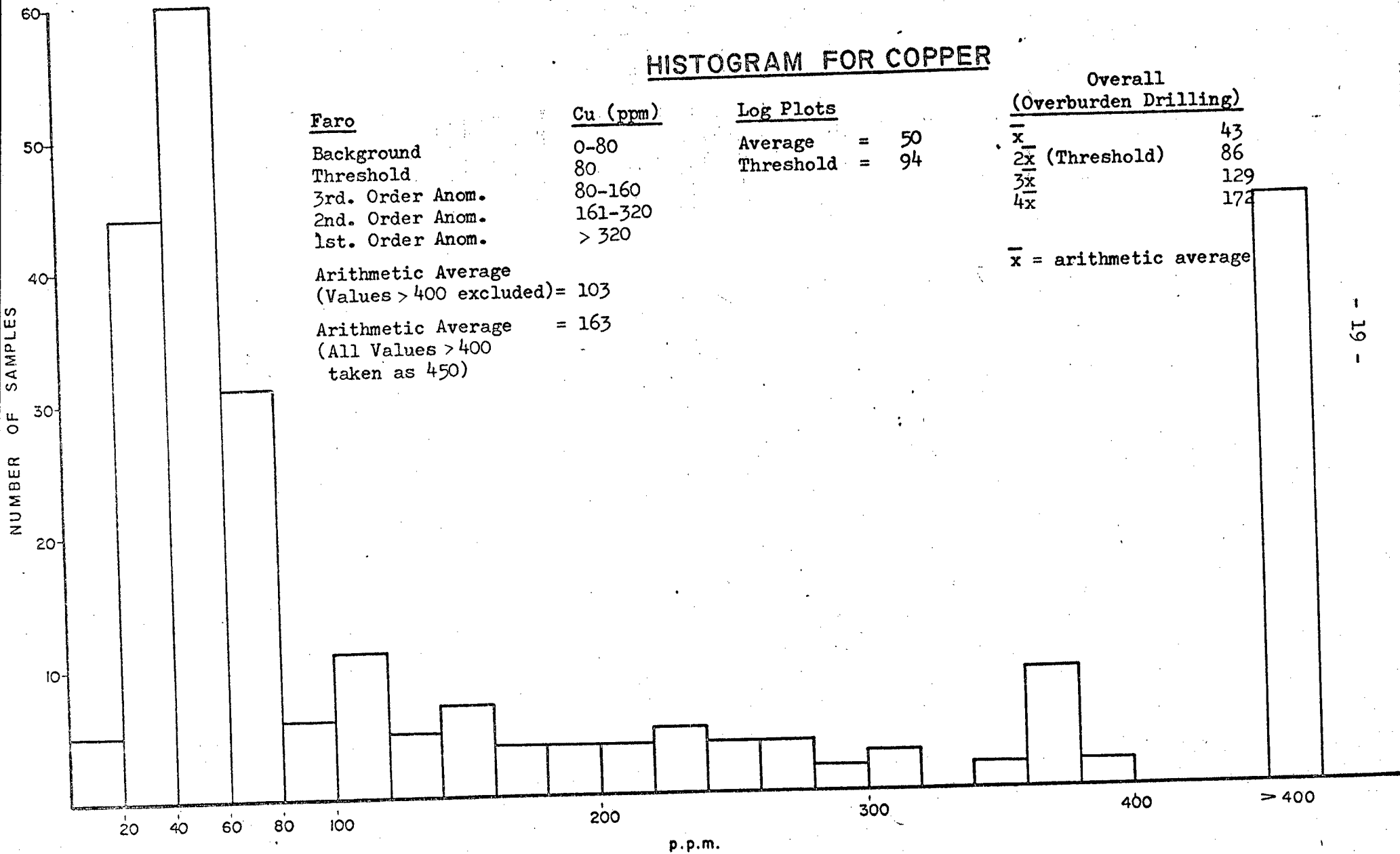
- 2) The lead content shows higher content in soils at two stations spatially closely related to the Faro #2 orebody, while in the other samples spatially removed from known mineralization the lead is concentrated in the overburden samples.
- 3) Zinc is concentrated in the soil samples spatially closely related to the Faro #2 orebody. Those samples believed to be spatially removed from the known mineralization show a concentration of zinc in the overburden material. The individual values and ratios of the element abundance in overburden to element abundance in soil is shown in the following table.
- 4) Soil geochem appears to be very specific in outlining these extensions of Faro #2, while high metal values in overburden can be traced downslope. Soil has not picked up metal values from overburden at STA 9. All overburden material in this hole is anomalous in Pb and Zn content. The soils at this station, however, only show a very weak lead anomaly, if in fact it can be considered an anomaly at all.
- 5) The metal ratios along 71-072 show directly increasing values of metal with depth in overburden over a mineralized zone. The values in the top (0-10 foot) sample interval were 94 ppm Pb and 960 ppm Zn, while at 60 feet, 5800 ppm Pb and 41500 ppm Zn was present.

#### Bedrock Orientation Survey

A bedrock orientation survey was performed by P.D.M. Bradshaw of Barringer Research Ltd. to determine if a halo of metal values in rock from drill cores could be detected around the Faro orebodies. The results of that study are summarized below. The values for these increments were picked from the histograms. These histograms were re-plotted here on log paper and reinterpreted. The reinterpreted values are compared with the average metal content, all tabulated on the histograms.

Anomalous Levels	<u>Provisional</u>				
	<u>Zn ppm</u>	<u>Cu ppm</u>	<u>Pb ppm</u>	<u>Hg ppm</u>	<u>Cd ppm</u>
Background	0-1000	0 - 80	0 - 300	0 - 300	0 - 3

# HISTOGRAM FOR COPPER



<u>Faro</u>	<u>Cu (ppm)</u>
Background	0-80
Threshold	80
3rd. Order Anom.	80-160
2nd. Order Anom.	161-320
1st. Order Anom.	> 320

Arithmetic Average  
(Values > 400 excluded) = 103

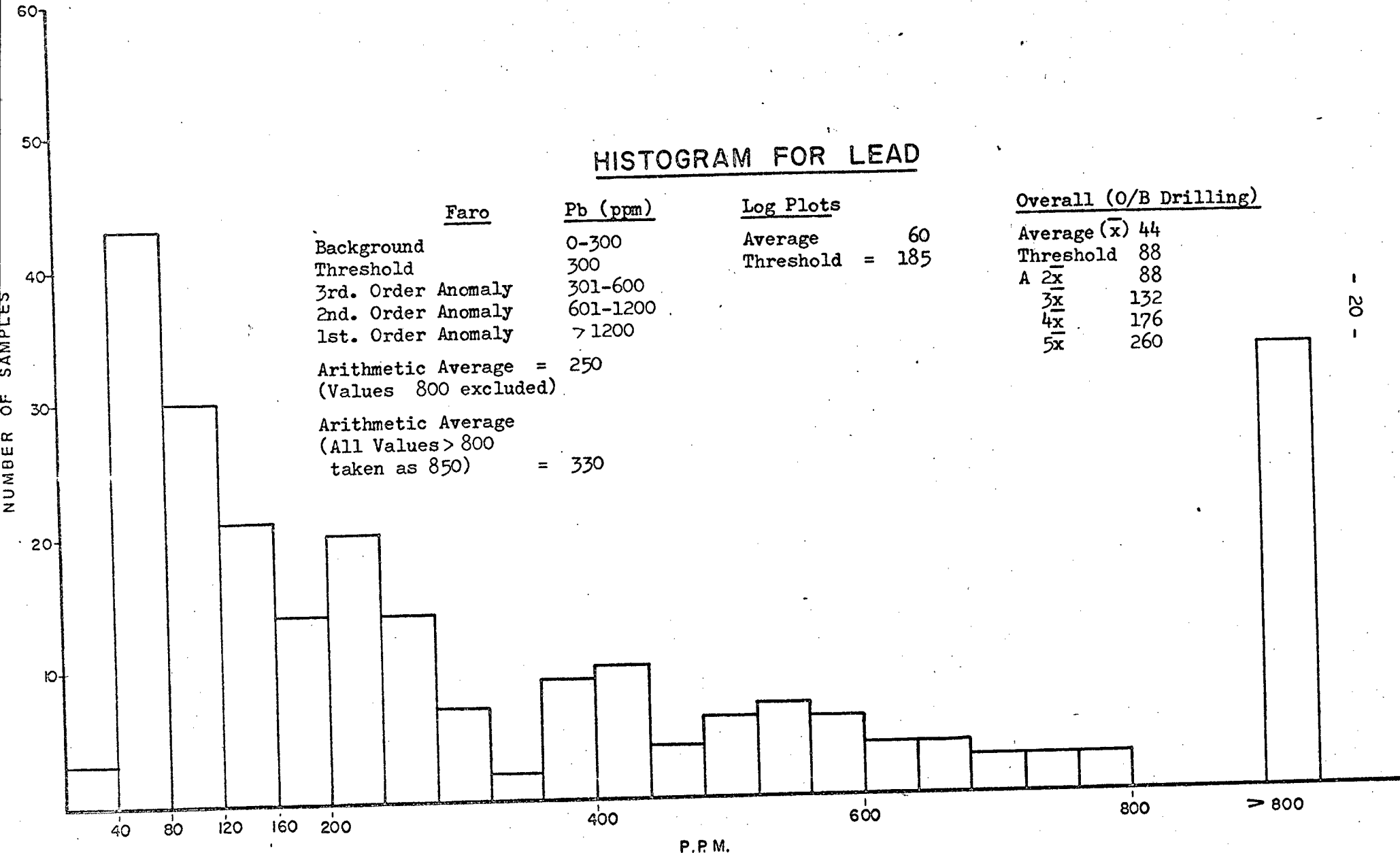
Arithmetic Average = 163  
(All Values > 400  
taken as 450)

<u>Log Plots</u>	
Average	= 50
Threshold	= 94

<u>Overall (Overburden Drilling)</u>	
$\bar{x}$	43
$2\bar{x}$ (Threshold)	86
$3\bar{x}$	129
$4\bar{x}$	172

$\bar{x}$  = arithmetic average

## HISTOGRAM FOR LEAD

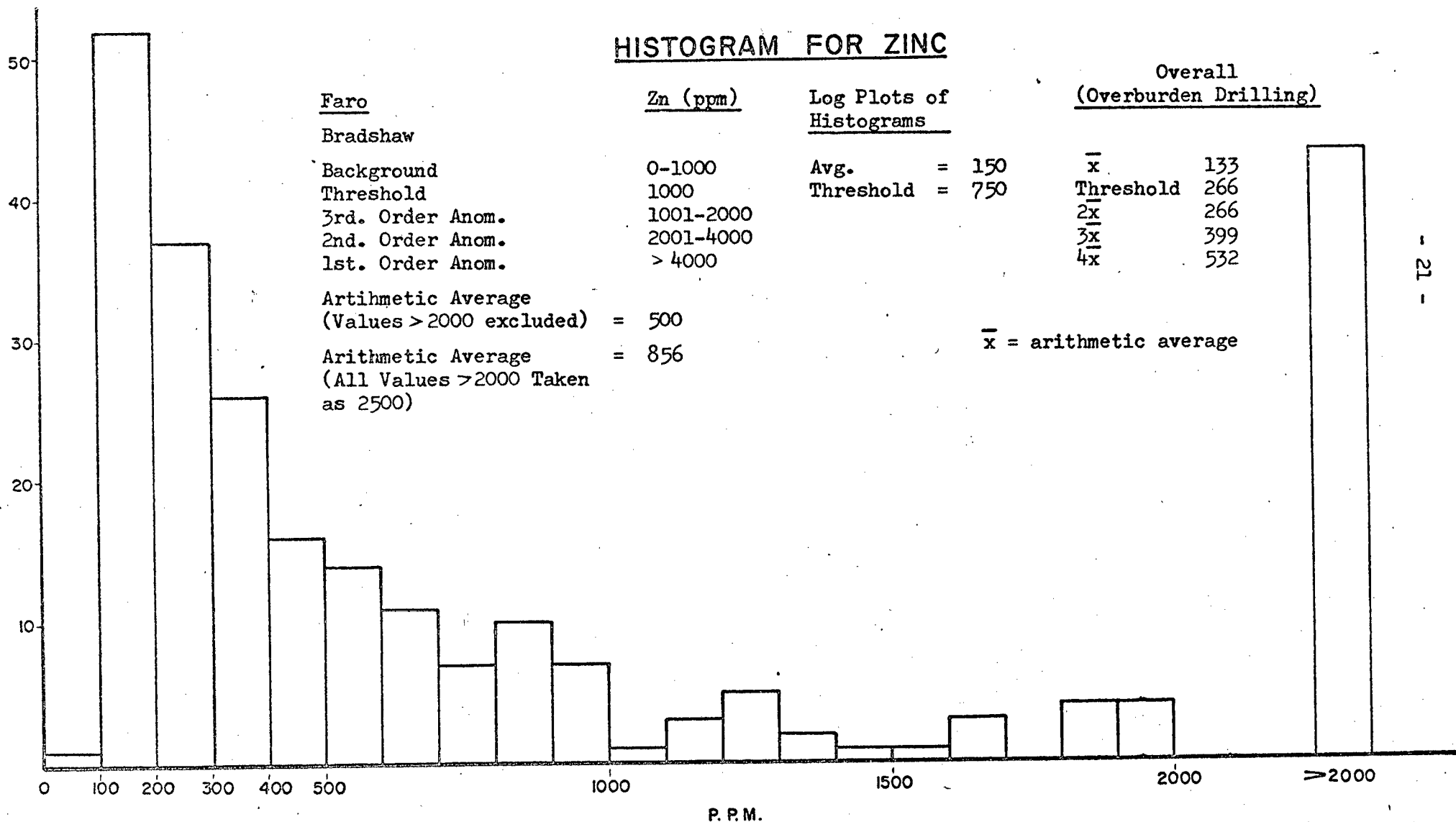


<u>Faro</u>	<u>Pb (ppm)</u>
Background	0-300
Threshold	300
3rd. Order Anomaly	301-600
2nd. Order Anomaly	601-1200
1st. Order Anomaly	> 1200
Arithmetic Average = 250 (Values 800 excluded)	
Arithmetic Average (All Values > 800 taken as 850) = 330	

Log Plots  
 Average = 60  
 Threshold = 185

Overall (O/B Drilling)  
 Average ( $\bar{x}$ ) 44  
 Threshold 88  
 A  $\frac{2x}{}$  88  
 $\frac{3x}{}$  132  
 $\frac{4x}{}$  176  
 $\frac{5x}{}$  260

## HISTOGRAM FOR ZINC



Faro

Bradshaw

Background

Threshold

3rd. Order Anom.

2nd. Order Anom.

1st. Order Anom.

Arithmetic Average  
(Values > 2000 excluded) = 500

Arithmetic Average  
(All Values > 2000 Taken  
as 2500) = 856

Zn (ppm)

0-1000

1000

1001-2000

2001-4000

> 4000

Log Plots of  
Histograms

Avg. = 150

Threshold = 750

Overall  
(Overburden Drilling)

$\bar{x}$  133

Threshold 266

$2\bar{x}$  266

$3\bar{x}$  399

$4\bar{x}$  532

$\bar{x}$  = arithmetic average

The following conclusions were reached by P.D.M. Bradshaw in Barringer's bedrock orientation survey at the Faro mine.

- 1) Spectrographic analysis of 22 sulphide and wallrock samples showed only copper, lead, zinc and possibly cadmium to be significantly higher in sulphides in the wall rock and show an even poorly recognizable wall rock dispersion.
- 2) Lead and zinc show detectable but erratic wall rock anomalies. The exact extent of the aureole cannot be estimated at this time because insufficient samples have been collected remote from the deposit, i.e. at distances greater than 400-500 feet. The present data do indicate, however, that lead in particular may form an irregular aureole using a threshold of 160 ppm, 200-400 feet wide about the deposit. Zinc is more erratic and less predictable. Both lead and zinc show the first order anomalous values remote from mineralization, and consequently their dispersion cannot be relied on for detailed interpretation although they may prove useful in indicating the general presence of the ore environment.
- 3) Copper shows a more restricted but more uniform wall rock dispersion. No first order copper values were found remote from mineralization. The copper dispersion is an average of 50 feet but varies between 9 and greater than 100 feet.
- 4) Cadmium shows a very restricted but very specific aureole.
- 5) Mercury shows the most regular wall rock aureole of all the elements tested, with a generally regular fall-off in concentration away from the orebody, up to a maximum distance of 170 feet.

Interpretation of the metal distribution around the orebody based on the reinterpreted values yields slightly different threshold values but yields the same conclusions.

### Conclusions

Evaluation of the soil, overburden, and bedrock geochemical orientation data shows:

- 1) The soil, till, and moss samples contained anomalous amounts of As, Au, Cd, Cu, Hg, Pb and Zn near known suboutcropping mineralization and all should be effective in locating near suboutcropping mineralized zones. Lead, zinc, and probably arsenic were more specific than other elements in outlining the mineralized zones than the other elements investigated.
- 2) Overburden geochemistry reveals a direct relationship between continuous intercepts of anomalous metal content in overburden material and a nearby source of the metals. Several patterns in the values have been observed at the Faro #2 orebody. Vertically the metal values decreased over 60 feet from 47300 ppm combined Pb and Zn at the bottom to 1054 ppm combined Pb Zn at the surface. Uphill from the orebody the overburden samples contain anomalous amounts of metals but in no apparent systematic distribution. Downhill from the Faro #2 orebody anomalous values were detected in the overburden samples. A systematic decrease in values is revealed in two holes, one 500 feet and the second 1500 feet below the Faro #2 zone.
- 3) The bedrock orientation survey revealed similar overall average metal contents as detected in analyses of individual rock types. However, a larger spread of values and higher threshold are indicated. Areas of high metal content in bedrock with values in excess of 94 ppm Cu, 185 ppm Pb, and 750 ppm Zn should be considered anomalous based on the data obtained at Faro.
- 4) Analysis of metal contents in specific rock types reveals that the Cu, Pb, and Zn contents are nearly identical. Because of the similar metal content in the various rock types, systematic differences in the metal content in the soil overlying specific rock types should not vary markedly.

APPENDIX II

Exploration Drilling - 1971

Atlas Copco (Modified)

Drilling and Sampling Procedure

Evaluation of Method

Advantages

Disadvantages

Mayhew 1000 Rotary Drill

Drilling and Sampling Procedure

Evaluation of Method

Advantages

Disadvantages

Longyear Model 38 (Diamond Drilling)

Evaluation of Rotary Drill Bits

Recommendations for Future Overburden Drilling

Drilling Costs

OVERBURDEN AND BEDROCK DRILLING PROGRAM - 1971

A drilling program was carried out to sample overburden and bedrock for chemical analysis and to identify bedrock for geologic mapping in areas of limited outcrop. Selected areas of interest were also later drilled by diamond drill.

The overburden-bedrock drilling was carried out by Big Indian Drilling Company of Calgary, Alberta. Two different drilling machines were used.

Diamond drilling was contracted to Arctic Drilling Company of Whitehorse, Yukon.

The details of the equipment and their performance are evaluated in the following report by J. Scheelar, Drilling Supervisor for Anvil Mining Corporation Limited.

---

EXPLORATION DRILLING - 1971

by

J. C. Scheelar

Drilling Supervisor

Anvil Mining Corporation Limited

Faro, Yukon

and

Uldis Jansons

The overburden and bedrock exploration drilling was done with three different drilling rigs. These rigs were:

- 1) A modified Atlas Copco, mounted on a Foremost track vehicle.
- 2) A Mayhew 1000, mounted on a Nodwell track vehicle.
- 3) A Longyear Model 38 diamond drill, mounted on a steel skid.

ATLAS COPCO (MODIFIED)

The machine was designed to drill with rotary percussion through the overburden and then 25 ft. of bedrock was cored with a diamond drill. The diamond drill used was a Boyles Bros. Model VAG with a #12 PG screw feed head, core size, AQ wireline.

Drilling and Sampling Procedure

The hole was advanced by drilling with rods to ten ft., at which time a sample of material encountered was retained; then the casing was advanced to depth. This procedure was repeated until bedrock was encountered. The diamond drill was then mounted on the back of the drilling rig and bedrock was cored.

### Evaluation of Method

#### Advantages:

The soil samples and rock cuttings obtained during this type of drilling, I feel, are superior to other methods due to the fact that the sample was taken from a virgin area isolated from the previous material sampled by casing.

#### Disadvantages:

- 1) Foremost track carrier.
- 2) Individual motors required for drills and mobilization equipment.
- 3) The use of external coupled casing.
- 4) The improper mounting of the diamond drill necessitating moving drilling machine to set up over the existing cased hole.
- 5) Inadequate hoisting equipment.

The use of flush coupled casing and a proper carrier would greatly increase the efficiency and versatility of this equipment.

### MAYHEW 1000 ROTARY DRILL

From late in June until the completion of overburden drilling in October 1971, a Mayhew rotary drill mounted on a Nodwell track vehicle was used. A selection of 4-3/4", 4-1/2" and 4-1/4" tri-cone bits were used. Drilling mud was used to build wall in the hole.

### Drilling and Sampling Procedure

Samples of soil and rock cuttings were taken from the mud tank at ten ft. intervals as the hole progressed. The mud tank was cleaned out and the next sample residue from these selected intervals was retained.

### Evaluation of Method

#### Advantages:

With the use of drilling mud and tri-cone bits, progress was quite acceptable. Mobility was good when equipment was operating properly. Moving time was usually less than 1/2 hr. between set-ups for holes spaced 1000 ft. apart.

#### Disadvantages:

The samples retained contained a considerable amount of drilling fluid.

When a drilling bit had to be changed, the mud tank was not sufficiently large to keep the drill hole full of fluid. Consequently, caving occurred and contaminated the following samples by materials from unprotected portion of the hole.

This rig was not suitable for drilling to depths in bedrock. Footage obtained from tri-cone bits was very low and costly, and progress was slow compared to diamond drilling.

### LONGYEAR MODEL 38 (DIAMOND DRILLING)

#### Arctic Drilling - Longyear Model 38

Diamond drilling commenced on October 31, 1971. To date, November 22, 66 ft. of overburden and 2606 ft. of bedrock has been drilled at a satisfactory rate.

Evaluation of Drill Bits

The life of bits used for overburden-bedrock drilling is evaluated. In overburden the tri-cone bits (either Varel or Walker MacDonald) averaged 131 ft. Several holes were drilled in bedrock to approximately 400 ft. The bit life in bedrock is evaluated for these.

<u>Hole</u>	<u>Average Footage Per Bit</u>	<u>Rock Type Encountered</u>
71-065A	18.46	Calc Silicate
71-066A	10.54	Calc Silicate
71-067	53.62	Calc Silicate
71-197	30.5	Biotite Phyllite
71-198	55	Biotite Phyllite
71-199	135	Biotite Phyllite
71-199A	48	Biotite Phyllite
71-200	50.62	Biotite Phyllite
71-201	106.25	Biotite Phyllite

Overall average was 34.43 ft. per bit in bedrock.

Tungsten carbide button bits were tried unsuccessfully - due to the inability to get sufficient weight on the bit. Approximately 5 ft. were drilled using this bit.

Evaluation of Contractor

Big Indian Drilling Company, Calgary, Alberta

The drilling rig, its carrier and the Nodwell water carrier at the start of use and despite a very considerable amount of repair, were still in very sad condition at completion of job.

The inexperience of some of the drill crew and lack of proper supervision was a contributing factor on lack of maintenance.

Big Indian provided good service in providing parts and equipment needed by field crews.

RECOMMENDATIONS FOR FUTURE OVERBURDEN DRILLING PROGRAMS

Recommended equipment for further exploration:

D-7 Cat - winch and dozer in good condition

Bombardier - service vehicle

Nodwell or equivalent - drill carrier

Longyear Model 38 diamond drill or equipment in place of Mayhew or other rotary drills.

Use of casing recommended:

HX or HW CSG - for collaring drill hole

NW CSG

BW CSG

BQ wireline coring equipment

The drill carrier should be equipped with proper outriggers and hydraulic jacks. This would cut down on moving and rigging-up time. The top of each hole should be cased. This will eliminate caving and contamination of samples. The ability to diamond core without shifting drill carrier is much to be desired, and on this particular set-up would be standard procedure.

DRILLING COSTS

Drilling costs of the rotary and coring are presented for comparison. The costs were calculated on a footage basis so that a direct comparison can be made. These calculated costs represent the total cost of the drill program. The cost of each item is calculated and represents figures that were used in applying the work requirements as presented to the Mining Recorder.

Rotary Drilling  
(Mayhew 1000)

Diamond Drilling

Costs Calculated Per Foot Of Hole Drilled

Contract	11.28	9.44
Camp	1.04	1.38
Supervisor	0.40	0.74
4 x 4	0.12	0.21
D - 7	1.38	1.86
Bombardier	0.13	0.39
Fuel	0.42	0.27
	<u>14.77</u>	<u>14.29</u>